REPORT DOCUMENTATION PAGE

Form Approved
OMB NO. 0704-0188

1. AGENCY USE ONLY (Leave Blank)	2. REPORT DATE	3. REPORT TYPE AND DATES COVERED
	November 07, 2005	Final Progress Report, August 15, 2002 – August 14, 2005

4. TITLE AND SUBTITLE
"Combustion Chemistry of Composite Solid Propellants Based on Nitramine and High Energetic Binders"

5. FUNDING NUMBERS
G

DAAD19-02-1-0373

6. AUTHOR(S)
Prof. O.P. Korobeinichev, Dr. A.A. Paletsky, Dr. A.G. Tereschenko, Dr. E.N. Volkov, P.D. Polyakov

7. PERFORMING ORGANIZATION NAME(S) AND ADDRESS(ES)
Institute of Chemical Kinetics and Combustion
Siberian Branch of Russian Academy of Sciences,
Institutskaya St., 3, 630090, Novosibirsk, Russia

8. PERFORMING ORGANIZATION REPORT NUMBER

9. SPONSORING / MONITORING AGENCY NAME(S) AND ADDRESS(ES)
U. S. Army Research Office
P.O. Box 12211
Research Triangle Park, NC 27709-2211

10. SPONSORING / MONITORING AGENCY REPORT NUMBER
43364.3-CH

11. SUPPLEMENTARY NOTES
The views, opinions and/or findings contained in this report are those of the author(s) and should not be construed as an official Department of the Army position, policy or decision, unless so designated by other documentation.

12 a. DISTRIBUTION / AVAILABILITY STATEMENT
Approved for public release; distribution unlimited.

12 b. DISTRIBUTION CODE

13. ABSTRACT (Maximum 200 words)
Chemical and thermal structure of flame of solid propellants based on nitramine (HMX or RDX) and azide polymer (GAP or BAMO-AMMO) has been investigated at pressure of 0.5 and 1.0 MPa by method of molecular-beam mass spectrometry and microthermocouple. Chemical flame structure of pure nitramines at atmospheric pressure has been obtained too. Burning rate has been measured. The probe method of sampling of species from flame allowing to detect products of propellant decomposition (including nitramine vapor) in the zone adjacent to the burning surface has been developed. Eleven species, including nitramine vapor, have been detected in the zone adjacent to the burning surface in the case of nitramine/GAP propellants. Experiments showed that there are two zones of chemical reactions in flame of nitramine/GAP propellants and one zone in flame of nitramine/BAMO-AMMO propellants. Species concentrations have been determined at different distances from the burning surface. Temperature profiles in the combustion wave of solid propellants have been measured. An extensive plateau on the temperature profiles was not observed. Data obtained can be used for creation and validation of combustion model for propellants on the basis of nitramine and azide polymer.

14. SUBJECT TERMS
HMX, RDX, GAP, BAMO-AMMO, flame structure of solid propellant, high pressure, molecular beam mass spectrometry

15. NUMBER OF PAGES
58

16. PRICE CODE

17. SECURITY CLASSIFICATION OR REPORT	18. SECURITY CLASSIFICATION ON THIS PAGE	19. SECURITY CLASSIFICATION OF ABSTRACT	20. LIMITATION OF ABSTRACT
UNCLASSIFIED	**UNCLASSIFIED**	**UNCLASSIFIED**	**UL**

“Combustion Chemistry of Composite Solid Propellants Based on Nitramine and High Energetic Binders”

Institute of Chemical Kinetics and Combustion
Siberian Branch of Russian Academy of Sciences

Grant Number DAAD19-02-1-0373
Proposal Number 43364-CH

FINAL PROGRESS REPORT

August 15, 2002, - August 14, 2005

Principal Investigator: Prof. O.P. Korobeinichev

Other Investigators:Dr. A.A. Paletsky
Dr. A.G. Tereschenko
Dr. E.N. Volkov
Graduate P.D. Polyakov

Table of Contents

List of Tables

List of Figures

The Research reported in this document has been made possible through the support and sponsorship of the U.S. Government through USA Army Research Office. This report is intended only for the internal management use of the Contractor and U.S. Government.

Scientific activities

Introduction

Studies of the combustion mechanism of composite propellants based on cyclic nitramine (HMX or RDX) with active binder (glycidyl azide polymer – GAP or copolymer bis-azido-methyl-oxetane/azido-methyl-methyl-oxetane – BAMO-AMMO) are of both practical and theoretical interest. Practical interest is motivated by the use of high energetic materials (EM) in solid propellants (SP), which provide good ballistic characteristics to propellants. At the same time, progress in the development of a model of propellant combustion strongly depends on the understanding of SP combustion mechanism and availability of combustion models for individual propellant ingredients (mainly oxidizers) based on realistic physicochemical processes and detailed kinetic mechanism of reactions in flame.

Experimental

The solid propellants flame structures at pressures of 0.1, 0.5 and 1 MPa was investigated using mass spectrometric probing (MSP) of flames of energetic materials (EMs) with molecular beam sampling (MBS) [1], a microthermocouple technique [2], and video-recording. In MSP of EM flames, the burning strand moves toward the probe at a rate exceeding the propellant burning rate with allowing consecutive sampling of species from all combustion zones, including the zone adjacent to the burning surface. The system of molecular beam MSP of EM flames detects both stable species and unusual species such as EM vapors. A time-of-flight mass spectrometer (TOFMS) was used to measure mass spectra of samples.

Experiments on combustion of solid propellants at different pressures were conducted in a high-pressure combustion chamber in an argon atmosphere. Propellant burning rates were determined by visualization of the motion of the propellant burning surface using video recording.

Quartz "sonic" probes with different wall thickness (Δr) were used. Combustion products were sampled through orifice with diameter of 30-40 μm at 0.5 MPa and 15-20 μm at 1.0 MPa. The opening angle of the internal cone of the probes was equal to ~ 40°. Three types of probes were used:

Probe 1: a thick-walled (Δr = 1.4 mm) probe with additional heating [3];

Probe 2: a thick-walled probe with wall thickness near the probe orifice less than in Probe 1 (Δr = 0.35 mm) without additional heating;

Probe 3: a thin-walled probe (Δr ~0.15 mm) without additional heating.

The main goal of using the probe with additional heating was to increase the temperature of the probe tip to a value slightly higher than the temperature of the propellant burning surface. This prevented plugging of the probe orifice due to nitramine vapor condensation on the inner walls of the probe near its tip. At the same time, this allowed detection of nitramine vapor in the low-temperature flame zone near the burning surface. In the case of Probes 1 and 2, failure of the probe orifice occurred if the residence time of the probe in flame exceeded 2 s. For Probe 3, the residence time of the probe in the flame should not exceed 0.6 s.

Investigation of the chemical structure of uncured composite propellants was conducted in argon at pressures of 0.5 and 1 MPa using quartz Probes 1, 2 and 3. The composition of products near the burning surface was measured using Probe 1 and Probe 2. The full flame structure was established using Probe 3.

Investigation of HMX and RDX flame structure at 0.1 MPa was conducted using an aluminum probe covered by thin layer of Al_2O_3. Probe has wall thickness of ~ 70 μm and diameter of inlet orifice of ~ 70 μm.

To obtain quantitative composition of combustion products, the mass-spectra of the main individual 12 species - H_2, H_2O, HCN, N_2, CO, NO, CH_2O, N_2O, NO_2, CO_2 and vapor of HMX and RDX (HMX_v, RDX_v) - were obtained and their calibration coefficients $k_{i/Ar}$ were measured: $k_{i/Ar} = \Delta I_{Ar}/\Delta I_i$, where ΔI_{Ar}, and ΔI_i are the changes of intensities of argon and i species peaks in calibration experiments. The mole fraction in our experiment was defined as

$$\alpha_i = I_i k_{i/Ar} / (\Sigma I_j k_{j/Ar}),$$

where $I_i=I_{i(exp)}-\Sigma I_{j(i)}$; I_i - mass peak intensity of *i* species; $I_{i(exp)}$ - initial experimental intensity; and $\Sigma I_{j(i)}$ - the intensity sum of all j species (except i species) which make contributions into $I_{i(exp)}$.

To identify HMX or RDX vapor special experiments on nitramines decomposition (evaporation) in the flow reactor [4] were carried out using MBMS setup and Probe 1.

The accuracy of measuring mole fractions of the final combustion products (H_2O, H_2, CO_2, N_2 and CO) was about 10%. The mole fractions of HCN, CO_2, N_2O, NO, NO_2 and nitramine vapor near the burning surface were measured with an accuracy of about 15%, and the mole fractions of CH_2O, N_2 and CO with an accuracy of about 30%.

The thermal structure of SP flame at 0.5 and 1 MPa was investigated using Π – shaped WRe(5%)-WRe(20%) ribbon thermocouples embedded in sample. The temperature of the final combustion products was corrected for heat loss by radiation [2]. The thermocouples were made by rolling wires of 15 and 50 μm in diameter. The thermocouples had a thickness (h) of ~ 6 and 15 μm and length of shoulders (l) of 1.2 and 3.0 mm at 0.5 and 1 MPa, respectively. The ratio l/h in our experiments was equal to ~ 200. The calculations in Ref. [2] show that at this l/h ratio, the temperature measurement error due to heat losses in the thermocouple shoulders does not exceed 2%. The temperature error in a single experiment was ± 25 K. The scatter in the temperatures of the final combustion products measured in different experiments was equal to ± 50 K.

The location of the burning surface was found from abrupt changes in most of the mass peak intensities at the moment of contact of the probe with liquid layer on the propellant surface. This was obviously related to density changes of the sampled products in a condensed to gas transition. In addition, the moment of contact of the probe with the burning surface was determined by video recording. Video recording was synchronized with mass spectrometric measurement [1].

Energetic Materials under Investigation and their Characteristics

1) HMX/GAP at 0.5 and 1.0 MPa;
2) RDX/GAP at 1.0 MPa;
3) HMX/BAMO-AMMO at 0.5 and 1.0 MPa;
4) RDX/BAMO-AMMO at 1.0 MPa;
5) RDX at 0.1 MPa;

6) HMX at 0.1 MPa.
7) HMX/GAP/HMDI (80/17.125/2.875 wt%) over a pressure range of 0.5-1.0 MPa.

Propellant samples were prepared by mixing of bimodal crystal of nitramine powder (coarse fraction with particle size of 150-250 μm and fine fraction with particle size of <20 μm in ratio of 50/50 wt%) and energetic binder.

The main characteristics of the propellants and its components are presented in Table 1, 2 and 3.

Results and discussions.

Burning rate of composite propellants

Burning rates of nitramine-based propellants with 20% of active binder (GAP or BAMO-AMMO) in comparison with burning rates of pure nitramines and data of Ref. [7] are presented in Figs. 1-4. Burning rate of the propellants is lower than burning rate of pure RDX or HMX. Comparison of our data on burning rate of nitramine/azide polymer propellants with data [7] showed that they are in good agreement with each other.

Flame Structure of HMX/GAP propellant at 0.5 MPa

An analysis of video records of the approach of the burning surface to Probe 3 at 0.5 MPa shows that a dark zone with an average width of 0.5 ± 0.1 mm exists near the burning surface of the propellant (Fig 5). The width of this zone was not constant during the propellant burning. On video records at 20-fold magnification, one can see the chaotic appearance of flame torches (3-5 torches simultaneously) with diameters of 0.5 – 1 mm on the burning surface (Fig. 6). The lifetime of a single torch is less than 0.04 s. Black particles (slightly protruded over the burning surface) with sizes of 0.1 – 0.15 mm are also observed on the burning surface. These particles obviously are partly decomposed GAP (Fig. 6). It is most likely that the formation of torches and temperature fluctuations are caused by the above mentioned non-homogeneity of the burning surface. Therefore, the width of the dark zone obtained from temperature and concentration profiles in different experiments can differ within 0.4-0.6 mm.

The composition of products near the burning surface of HMX/GAP propellant is not reproduced from experiment to experiment at a pressure of 0.5 MPa. The main difference observed is variation in the mole fraction of HMX_v from 0.1 to 0.27. Depending on the variation of HMX vapor concentration, the NO concentration varied from 0.24 to 0.10, the NO_2 concentration from 0.03 to 0.14 and the H_2O concentration from 0.20 to 0.06, respectively. The concentrations of the remaining products changed slightly. The main reason for this irreproducibility is probably the non-homogeneity of the burning surface, i.e., the presence of black particles on the burning surface revealed by video recording. These particles move slowly over the burning surface and are probably partly decomposed GAP. Therefore, the observed irreproducibility of the composition of products near the burning surface is mainly due to the presence or absence of "GAP particle" on the burning surface near the tip of the probe. This implies that it is better to use averaged data (Table 4) on the composition of products near the burning surface for further application and validation of the HMX/GAP combustion model. In addition, in a zone near the surface, mass peaks 39, 41, 42, and 43 were recorded. Mass peak 43 is probably relates to HNCO and/or HCNO. Part of mass peak 42 relates to HMX vapor and the remaining part is probably relates to CH_2N_2 and HCNO+HNCO. Mass peaks 39 and 41 were not identified. It was established that these peaks decreased with increase in distance from the burning surface. We assume that the products of GAP combustion and/or thermal decomposition are responsible for these peaks. These peaks were not taken into consideration in the calculations of the combustion product composition.

The composition of HMX/GAP combustion products at 0.5 MPa at a distance larger than 1.2 mm from the burning surface is very close to that at thermodynamic equilibrium (Table 4, Equil).

The HMX/GAP flame structure at 0.5 MPa obtained using Probe 3 is presented in Fig. 7. The chemical and thermal structures were obtained in different experiments. The temperature profile is the result of averaging of several profiles obtained in different experiments and subsequent smoothing. The width of the zone of HCN and NO consumption obtained in mass spectrometric measurements coincides with the dark zone width measured using video recording. In the dark zone of width ~ 0.5 mm, two zones of chemical reactions were detected. In the first (Fig. 7a), narrow, zone 0.1 mm wide

(adjacent to the burning surface), complete consumption of HMX_v, and NO_2 and partial consumption of CH_2O with formation of NO, HCN, and N_2O occur. The concentrations of CO, N_2, and H_2 change only slightly. The temperature in this zone increases from 600 to ~ 970 K. Next, at a distance of 0.1-0.5 mm, consumption of N_2O, CH_2O, HCN, and NO (Fig. 7b) with formation of H_2, CO, and N_2 takes place (Fig. 7c). The temperature increases from 970 to 2000 K. Unlike the experiments described in Ref. [7], which showed the existence of an extensive plateau on the temperature profile of HMX/GAP flame at 0.5 MPa (at a temperature of ~ 1300 K), no such plateau was found in our experiments (Fig. 7). But temperature profiles have a peculiarity at a distance of ~ 0.13÷0.25 mm from the burning surface, that relates to decrease of temperature gradient. Thus, the NO, HCN, and N_2O concentration profiles have maximum at L ~ 0.12 mm. At distances larger than 0.5 mm, a luminous zone begins, in which there is further consumption of HCN. In the experiment whose results are presented in Fig. 7, concentration profiles were measured only to ~ 0.7 mm. At this distance, HCN is not completely consumed and the temperature reaches ~ 2300 K. In the experiments in which flame structure was investigated at large distances from the burning surface, the width of HCN consumption zone was significantly greater than that of the remaining products and was equal to ~1.0 mm. The H_2O and CO_2 concentrations changed slightly in the whole flame zone. The H_2 concentration maximum is reached at L = 0.35 mm, whereas the maxima of concentrations of CO and N_2 concentrations are observed at L = 0.55 mm. A possible reason for this is that the diffusion coefficient of H_2 is higher than those of remaining combustion products. Element content profiles in HMX/GAP propellant flame at 0.5 MPa calculated without taking into account diffusion fluxes of species are presented in Fig. 8. The maximum deviations of N and H contents are ~ 25-30%. The oxygen content coincides with the initial amount over the entire flame zone. The largest deviation (~ 40%) from the initial element content is observed for carbon. In a zone ~ 0.1 mm wide adjacent to the burning surface there is a steep gradient of species concentrations; therefore, the element content in this zone can differ from initial one. However, the concentration gradient decreases at distances larger than 0.1 mm but the amounts of C, H, and N still differ from the initial ones. It can be assumed that a decrease in the amounts of C and H near the burning surface is due to the presence of unidentified

gaseous products of GAP gasification. This assumption explains the nature of the dependence of C and H content on the distance from the burning surface.

Flame Structure of HMX/GAP and RDX/GAP propellants at 1.0 MPa

Compositions of products near the burning surface of HMX/GAP and RDX/GAP propellants at 1 MPa are presented in Table 4. Mass fraction of HMX_v (RDX_v) in identified products near the burning surface (L=0 mm) at a pressure of 1 MPa comprises ~ 70% (~ 80%). Taking into account that mass fraction of nitramine in propellants is equal to 80%, this means that significant part of initial nitramine transfers to the gas phase as vapor. Quantitative analysis of the compositions of gasification products for investigated propellants based on different nitramines (RDX and HMX) showed that mole fraction of H_2O, N_2, and NO in the case of RDX/GAP is significantly less in comparison with HMX/GAP propellant, but mole fraction of NO_2 and nitramine vapor (RDX_v) are larger.

The final combustion products of HMX/GAP and RDX/GAP propellants at 1 MPa at a distance ~1 mm from the burning surface are very close to those at thermodynamic equilibrium (Table 4, Equil).

Flame structure of HMX/GAP propellant at 1 MPa and content of elements in flame zone are presented in Fig. 9 and Fig. 10. At a pressure of 1 MPa (as in the case of 0.5 MPa) two zones of chemical reaction were found. The first zone is a zone of consumption of HMX vapor and NO_2 with formation of NO, HCN, CO, H_2 and N_2. In the second zone, consumption of N_2O, CH_2O, NO and HCN with further formation of CO, H_2 and N_2 occurs. Temperature in the first zone grows from 640 to ~ 1100 K, and in the second zone – from ~ 1100 to ~ 2200 K. As in the case of 0.5 MPa, at a pressure of 1 MPa the zone of HCN consumption is wider than those of other species. Element content profiles (Fig. 10) were calculated without accounting for diffusion fluxes of species. The maximum deviations of N and O contents are ~ 15% from initial amount. For C and H elements maximum deviations comprise ~ 20% and ~ 25%, respectively.

Flame structure of RDX/GAP propellant at 1 MPa and content of elements in flame zone are presented in Fig. 11 and Fig. 12. Profiles of species concentrations in

flames of RDX/GAP and HMX/GAP propellants are similar; there are only some, mostly quantitative differences between them.

Two main zones of chemical reactions in flame of nitramine/GAP propellants at a pressure of 1 MPa were observed. In the first low-temperature (dark) zone, consumption of nitramine vapor and reaction of CH_2O oxidation by NO_2 mainly occur. Most part of NO_2 and nitramine vapor is consumed at a distance less than ~ 0.1 mm from the burning surface. This leads to formation of NO, CO, H_2 and N_2. In the second high-temperature zone, the main reaction is reaction of HCN oxidation by NO, leading to formation of such final products as CO, N_2 and H_2. It was shown in Refs. [9, 10] that this reaction is main reaction in high-temperature zones of RDX [9] and HMX [10]. Thus, in nitramine/GAP propellant flames the same reactions (as in the case of pure nitramines) play lead role.

Thermal Structure of HMX/GAP and RDX/GAP propellants at 1.0 MPa

Preliminary experiments on combustion of samples of RDX/GAP propellant at pressure of 0.5 MPa showed that burning surface of the propellant is inhomogeneous and contains significant amount of carbonaceous particles. This fact did not allow us to conduct experiments on studying of chemical structure of RDX/GAP propellant at 0.5 MPa.

Fig. 13 presents averaged and smoothed temperature profiles for HMX/GAP and RDX/GAP propellants at a pressure of 1 MPa. Experimentally measured value of final flame temperature for both propellants is equal to ~ 2580 K. But the distance, at which this final temperature is achieved, differs and comprises 0.7 mm for HMX/GAP and 0.4 mm for RDX/GAP. Calculation of thermodynamic equilibrium at a pressure of 1 MPa using “Astra” code [11] showed that adiabatic temperature for HMX/GAP propellant is equal to 2608 K (in the case of RDX/GAP T_{ad} = 2617 K). Small differences of experimental values of final temperature from calculated ones are in limits of accuracy of thermocouple technique.

The length of the “plateau” for RDX/GAP propellant flame at 1 MPa is less than that in similar measurement [7]. However, it is more extensive than that for HMX/GAP flame at the same pressure (Fig. 13).

Comparison of obtained temperature profiles with data [7], showed that there are two main distinctions between them. The first distinction is a presence of extensive

plateau (at a temperature of ~ 1300 K) on profiles obtained in Ref. [7]. The second distinction concerns temperature of final products: according to our measurements for both propellants it is equal to ~ 2580 K, while in Ref. [7] final temperature comprised only 2320 and 2360 K for HMX/GAP and RDX/GAP propellants at 1.0 MPa, respectively. A possible reason for the difference between our data and the data of Ref. [7] is obviously connected with differences in GAP (elemental composition, enthalpy of formation) and propellant density. The density of the propellant used in Ref. [7] was 88% of the calculated maximum density versus ~98% in our case.

Temperature profiles for cured HMX/GAP propellant.

Fig. 14 shows combustion behavior of cured HMX/GAP propellant at pressures of 0.5 and 1.0 MPa. These images were obtained during execution of temperature measurements. Combustion behavior of cured HMX/GAP propellant differs from combustion behavior of uncured propellant. In the case of cured HMX/GAP propellant at a pressure of 0.5 MPa (Fig. 14a) burning surface is covered by carbonaceous fibers protruding in gas phase. Increase of pressure to 1.0 MPa (Fig. 14b) resulted in decrease of quantity of these fibers, but they still present on the burning surface. On the burning surface of uncured HMX/GAP propellant there were observed only carbonaceous particles. Transition from carbonaceous particles to carbonaceous fibers obviously relates to curing of propellant.

Presence of carbonaceous fibers on the burning surface did not allow us to conduct experiments on studying of chemical structure of cured HMX/GAP propellant.

Temperature profiles without correction for heat losses by radiation (individual experimental profile) in flame of cured HMX/GAP propellant for three different pressures (0.5, 0.7 and 1.0 MPa) are presented in Fig. 15. The length of the flame zone (as it was expected) decreases with increase of pressure. Final flame temperature, which is equal to ~2400 K (with correction for heat losses by radiation), is reached at ~ 2 mm for pressure of 0.5 MPa and ~ 1 mm for 1.0 MPa. According to temperature profile obtained at 0.5 MPa there are strong fluctuations of temperature at distances of 1-2 mm from the burning surface. These fluctuations relate to non-uniformity of the burning surface (presence of carbonaceous fibers). Temperature profiles obtained at 1 MPa are

close to each other (Fig.17). These profiles do not have strong fluctuations similar to those at 0.5 MPa, because quantity of carbonaceous fibers on the burning surface at 1 MPa is significantly less than at 0.5 MPa.

Comparisons of temperature profiles for cured HMX/GAP propellant with profiles for uncured propellant (our previous data) and with profiles of Ref. [7] for cured propellant are presented at Figs. 16 and 17 for pressures 0.5 and 1 MPa respectively. Curing of propellant leads to decrease of final temperature of flame and to widening of flame zone. Density of cured propellant used in present investigation (1.53 g/cm^3) is very close to data of [7] (1.52 g/cm^3). However, in contrast to our observations Zenin did not observe any carbonaceous residue on the surface of the propellant. Absolute value of final temperature at a pressure of 1.0 MPa for cured propellant is by ~200 K less than that for uncured propellant (our data) and is close to Zenin's data for cured propellant [7] (Fig. 17). However contrary to Zenin's data we did not observe any plateau on temperature profiles for cured HMX/GAP propellant at 1.0 MPa.

Flame structure of HMX/B-A flame at 0.5 MPa

Video recording has shown that during combustion of HMX/B-A propellant at 0.5 MPa the carbonaceous carcass almost completely covers the burning surface of propellant. Parts of this carcass detached from the surface and then burned in gas phase. A carbonaceous residue remained on a sample holder after the experiment.

Two temperature profiles (with radiation correction) in the combustion wave of HMX/B-A propellant at 0.5 MPa, which were obtained in different experiments, are presented in Fig.18 in comparison with data of Ref. [7]. The final flame temperature, which is equal to 2400 K, was achieved in our experiments at a distance of 1.5-1.7 mm. This value is less than equilibrium temperature (2503 K) by 100 K. We suppose that incompleteness of combustion at a pressure of 0.5 MPa relates to the presence of the carbonaceous carcass on the burning surface. Temperature curves, obtained in different experiments, are characterized by strong temperature fluctuations (up to 600 degrees) at a distance of 0.5-1.7 mm from the burning surface. Every single temperature profile, obtained in our investigation, oscillates near the temperature profile presented in Ref. [7], which was obtained as a result of averaging of several profiles. Final flame temperature measured in our investigation is higher than that in Ref. [7] by ~ 280 K. Strong

temperature fluctuations are most likely due to torch combustion of the propellant and non-uniformity of the burning surface. Composition of combustion products can significantly differ depending on position of torch above the burning surface. Similar to data of Ref. [7], at a distance of 0.2-0.5 mm from the burning surface a plateau (region with slight temperature growth) was observed (at a temperature of ~ 1100 K).

Fig.19 shows temperature profiles near the burning surface of HMX/B-A propellant at a pressure of 0.5 MPa (obtained in different experiments) in comparison with data of Ref. [7]. Burning surface temperature, which was determined by the first slope break on temperature profile, seemingly corresponds to the interface between condensed phase and foam layer. Farther there is the second (less pronounced) slope break, which most likely corresponds to transition of thermocouple from the foam layer to the gas phase. Width of the foam layer was ~ 0.06 mm. Surface temperature determined from our experiments is higher than data of Ref. [7] by ~ 50 K and comprises ~ 655 K.

Chemical structure of HMX/B-A flame at a pressure of 0.5 MPa is presented in Fig.20. Table 5 shows species concentrations (in mole fractions) in flame of HMX/B-A propellant at 0.5 MPa at different distances from the burning surface. It is noteworthy that the fluctuations of mass peaks corresponding to HCN, NO, N_2O at distances from the burning surface larger than 0.7 mm were not taken into consideration when determining propellant flame structure. Therefore obtained flame structure relates to a single torch. Only one zone of chemical reactions in flame of HMX/B-A propellant was revealed at a pressure of 0.5 MPa in contrast to HMX/GAP propellant. HMX vapor and CH_2O were found near the burning surface of HMX/B-A propellant only in trace concentrations, which are close to accuracy of measurements, and NO_2 was not observed at all. Narrow zone, which is characterized by consumption of HMX vapor, NO_2 and CH_2O, was not observed near the burning surface of HMX/B-A propellant. It possibly relates to presence of carbonaceous carcass on the burning surface and sufficiently high value of burning surface temperature (655 K for HMX/B-A, 603 K for HMX/GAP). Mole fraction of CO (0.12) near the burning surface of HMX/B-A propellant is higher than in the case HMX/GAP. It may indicate that chemical reaction in the condensed phase occurs more intensively in combustion of HMX/B-A propellant. Width of consumption zone for main intermediate combustion products is equal to ~ 0.6 mm. Monotonic consumption of NO

and N_2O starts from the burning surface. However, concentration of HCN has a plateau, which length coincides with length of the plateau on temperature profiles. Most likely, it means that together with reactions, in which HCN consumes, reactions with formation of HCN occur. As HCN is one of the main product of laser-supported decomposition of B-A (mole fraction is ~ 0.19 [12]), then it can be assumed that formation of HCN occurs also as a result of heterogeneous decomposition of partly reacted (elimination of N_2) copolymer B-A in the condensed phase.

New species, such as HCNO and (or) HNCO (m/e=43), CH_2N_2 (m/e=42) and C_2N_2 (m/e=52), were revealed near the burning surface in small concentrations (with mole fractions ~ 0.01). Calibration coefficients for these species were taken the same as for N_2O.

Significant distinctions between composition of final combustion products of HMX/B-A propellant and equilibrium composition at 0.5 MPa are observed for hydrogen-containing products (Table 5). The main hydrogen-containing product in composition of final products is H_2O, and in equilibrium composition – H_2. Possibly it relates to incomplete burning of propellant sample, which is confirmed by the presence of carbonaceous residue after its burning.

Content of C and H elements (per 1000 g) in products near and far from the burning surface ($C_{12.8}H_{23.3}N_{29.6}O_{25.6}$) is substantially less than initial content of these elements in HMX/B-A propellant ($C_{17.6}H_{33.1}N_{27.7}O_{23.0}$). It is in agreement with presence of carbonaceous residue after propellant burning.

Flame structure of HMX/B-A propellant at 1.0 MPa

Video recording revealed presence of carbonaceous particles on the burning surface upon combustion of HMX/B-A and RDX/B-A propellants at a pressure of 1 MPa. In the case of HMX-based propellant, fine carbonaceous particles covered almost entire burning surface (Fig. 21a). In the case of RDX/B-A propellant (Fig. 21b), on the burning surface there was observed formation of big carbonaceous flakes, which detached from the burning surface and then burned in gas phase. After detachment of a big particle on the burning surface there were observed regions free of carbonaceous carcass.

Fig.22 shows two temperature profiles (with correction for radiation of thermocouple) for HMX/B-A propellant, which were measured in different experiments

at a pressure of 1.0 MPa, in comparison with data of Ref. [7]. Final temperature in flame of the propellant, which is equal to 2500 K, was achieved at a distance of 0.6-1.1 mm. This value coincides with adiabatic temperature (2512 K) and exceeds experimental data of Ref. [1] by ~ 200 K. Nonreproductivity of temperature profile measurements is connected with influence of carbonaceous particles on results of measurements as well as with torch combustion of the propellant and non-uniformity of the burning surface. In contrast to data of Ref. [7] the plateau at a temperature of about 1250 K is absent in our temperature profiles.

Presence of carbonaceous particles on the burning surface did not allow to analyze the zone adjacent to the burning surface.

Figure 23 shows flame structure of HMX/B-A propellant at a pressure of 1.0 MPa. Species concentrations in flame of HMX/B-A propellant at 1.0 MPa at different distances from the burning surface (in mole fractions, without species with concentration less than 0.02) are presented in Table 6. As in the case of 0.5 MPa there is only one zone of chemical reactions in the flame of HMX/B-A propellant at a pressure of 1 MPa (in contrast to HMX/GAP flame), in which consumption of HCN, NO and N_2O occurs. NO_2, CH_2O and HMX vapor were not observed in the product composition near the burning surface of HMX/B-A propellant. Width of zone of monotonic consumption of main gasification products (HCN, NO and N_2O) comprises ~ 0.6 mm, and width of complete consumption of HCN is equal to ~ 1.5 mm. With increase of pressure to 1.0 MPa the width of flame zone decreases, concentrations of HCN, NO and N_2O in gas phase near the burning surface became several times less, and concentrations of H_2 and N_2 became higher than those at 0.5 MPa. This probably relates to the intensification of reactions in condensed and in gas phases at a pressure of 1 MPa in comparison with a pressure of 0.5 MPa.

There is observed substantial deviation of the final combustion product composition of HMX/B-A propellant at 0.5 and 1.0 MPa from equilibrium product composition as regards the concentration of hydrogen-contained species (Table 6). H_2 concentration in final combustion products increased by ~ 1.8 times, and concentration of H_2O decreased by 1.5 times upon increase of pressure from 0.5 MPa to 1.0 MPa. Thus, measured concentrations of hydrogen-containing combustion products at 1 MPa still did not achieve those in equilibrium composition, but approached to them.

Flame structure of RDX/B-A propellant at 1.0 MPa

Temperature profile (with correction for radiation of thermocouple) for RDX/B-A propellant at a pressure of 1.0 MPa in comparison with data of Ref. [7] is presented in Fig. 24. Final temperature in flame of the propellant, which is equal to 2560 K, was achieved at a distance of ~1.5 mm. This value coincides with adiabatic temperature (2522 K) and exceeds experimental data of Ref. [7] by ~ 280 K. In contrast to data of Ref. [7] the plateau at a temperature of about 1250 K is absent in our temperature profiles. There was observed only a slight decrease of temperature gradient, which increased again at a distance of ~ 0.25 mm.

Figure 25 shows flame structure of RDX/B-A propellant at a pressure of 1.0 MPa. Species concentrations in flame of RDX/B-A propellant at 1.0 MPa at different distances from the burning surface (in mole fractions) are presented in Table 7. NO_2, CH_2O and RDX vapor were not observed in the product composition near the burning surface of RDX/B-A propellant. Width of zone of monotonic consumption of main gasification products (HCN, NO) comprises ~ 0.7 mm, and width of complete consumption of HCN is equal to ~ 1,5 mm. There is observed substantial deviation of the final combustion product composition of RDX/B-A propellant at 1.0 MPa from equilibrium product composition as regards the concentration of hydrogen-contained species. Measured concentrations of hydrogen-containing combustion products at 1 MPa did not achieve those in equilibrium composition.

Flame Structure of HMX at 0.1 MPa in Air

HMX combustion at atmospheric pressure in an inert atmosphere is nonstationary. [13-15]. The profiles of species concentrations without averaging in HMX flame at air pressure of 0.1 MPa are presented in Fig. 26. Pellets of HMX had diameter of 8 mm, length of 6-8 mm and density of 1.80±0.01 g/cm^3. Burning rate of HMX pellets was equal to ~ 0.65 mm/s. Fig. 26 shows that there are oscillations on concentration profiles. HMX vapor oscillations were observed near the burning surface at a distance up to 0.5 mm. Far from the burning surface at a distance of 1.5-3 mm periodic oscillations of combustion products in antiphase were observed: concentrations of HCN and NO simultaneously increased from mean value and CO and N_2 concentrations decreased.

Duration of oscillations is equal to ~ 0.1 s, and their frequency is ~ 4 Hz. Amplitude of oscillations is different.

Averaged smoothed data on species mole fractions in HMX flame are presented in Fig. 27. HMX flame at 0.1 MPa has two-zone structure. In the first zone at a distance from the burning surface less than ~ 0.8 mm consumption of HMX vapor, NO_2, CH_2O and partial consumption of N_2O with formation of H_2, H_2O, CO, N_2, CO_2, HCN and NO (it is likely that along with NO formation near the surface its consumption occurs) take place. In the second flame zone at a distance of 0.8-1.5 mm from the burning surface intense consumption of HCN and NO with formation of N_2, CO, and H_2 occurs.

Composition of products near the burning surface for self-sustained combustion at a pressure of 0.1 MPa in comparison with that from Ref. [16] for laser-supported combustion is presented in Table 8. It can be seen that in self-sustained combustion HCN, CO and NO_2 concentrations near the burning surface are significantly lower and concentrations of NO and H_2O are significantly higher than in laser-supported HMX combustion. Mass fraction of HMX vapor near the burning surface is equal to ~ 30%.

Composition of final combustion products of HMX at 0.1 MPa does not correspond to equilibrium composition as it contains NO in amount equal to ~ 0.07.

The result of subtraction of mass spectrum of combustion products in the end of the first zone of HMX flame at 0.1 MPa (at a distance of ~ 0.5 mm) from mass spectrum of products near the burning surface is presented in Fig.28. Besides the main peaks in Ref. [16] at ionization energy of 22 eV the following peaks with low intensity: 42, 43, 45, 47, 54, 70, 81, 97 were detected near the burning surface. In our investigation at electron energy of 70 eV these peaks also were observed, but in addition to them the following mass peaks: 40, 41, 56, 67, 75 were detected. We suppose that peaks 42 and 43 relate to HNCO and HCNO. Low-intensity peaks 40, 41, 43, 45 were not identified and therefore were not accounted for in determination of flame structure. In the end of the first zone the mass peak 52 was detected.

Flame Structure of RDX at 0.1 MPa

Experiments on combustion of RDX was conducted in argon atmosphere at pressure of 0.1 MPa. Density of the pellets was equal to 1.7 g/cm^3 (94% of TMD). In all experiments during ignition of RDX a formation of big bubbles on the pellet surface

was observed. In some experiments these bubbles completely disappeared after ignition of pellet, in others they remain on the pellet surface during the combustion. When bubbles were presented on the burning surface, combustion of pellet was unstable or ceased in several seconds after ignition (incomplete burning of pellet). In other cases (~ 40% of experiments) regular combustion (without bubbles) with burning rate of ~ 0.27 mm/s was observed.

Chemical structure of RDX flame at a pressure of 0.1 MPa is presented in Fig. 29. Near the burning surface of RDX at 0.1 MPa exists narrow zone of RDX vapor and NO_2 consumption with width of ~ 0.15 mm. N_2O consumption zone is wider than zone of consumption of RDX vapor, width of this zone comprises ~ 0.3 mm. Zone of complete consumption of HCN comprises about 1 mm. According to experiment NO is not consumed completely even at a distance of ~ 2 mm. Mole fraction of NO in final combustion products is equal to ~ 0.05. RDX flame structure at 0.1 MPa was determined without taking into account profiles of intensities of weak mass peaks (42 and 43). Mass-peaks 42 and 43 were supposed as CH_2N_2 and HCNO+HNCO correspondingly.

On the basis of the experimental data, modeling of chemical structure of RDX flame was performed. Modeling was conducted using gas-phase mechanisms for RDX combustion. PREMIX/CHEMKIN software was used.

Chemical structure of RDX flame obtained using experimentally measured composition of products near the burning surface (Table 9) as a boundary condition is presented in Fig. 30. Comparison with experimental data showed that modeling can satisfactorily describe concentration profiles of such species as N_2, CO, HCN, NO, H_2O, H_2, CO_2 and RDX vapor. For NO_2, N_2O and CH_2O agreement between calculated and measured concentration profiles is not so good.

Equation of chemical reaction corresponding to experimentally measured product composition near the burning surface is given as:

$$RDX_C \rightarrow 0.39RDX_v + 1.22NO + 0.9H_2O + 0.9HCN + 0.266N_2 + 0.64CO + 0.266H_2 +$$
$$+ 0.266NO_2 + 0.16CO_2 + 0.213N_2O + 0.053CH_2O + 0.034(HCNO+HNCO) + 0.086CH_2N_2$$

where RDX_C – RDX in condensed phase.

Heat release of this reaction is -31 cal/g. According to [17] this value is –84 cal/g. The disagreement is probably due to both experimental errors (at thermocouple and mass spectrometric investigations) and errors at data processing.

Main results and conclusions

For the first time, flame structure of composite propellants was experimentally determined at such a high pressure (up to 1 MPa) using molecular beam mass spectrometry.

Eleven species (H_2, H_2O, HCN, N_2, CO, CH_2O, NO, N_2O, CO_2, N_2O and nitramine vapor) in flame of solid propellants based on nitramine and GAP (80/20 wt%) at a pressure of 0.5 and 1 MPa and in flame of pure nitramines (RDX and HMX) at a pressure of 0.1 MPa were found.

Mole fraction of nitramine vapor near the burning surface was determined for both composite propellants and pure nitramines. The calibration coefficients for nitramine vapor were measured at a pressure of 0.1 MPa. It was shown that in the case of solid propellant combustion at high pressure the significant part of initial nitramine transfers to the gas phase as vapor. In the case of combustion of pure nitramines at 0.1 MPa mass fraction of RDX vapor near the burning surface was equal to 0.38 from initial nitramine and 0.31 - for HMX.

Burning rates of the propellants as well as temperature and concentration profiles in propellant combustion wave were measured. An extensive plateau on the temperature profiles of the nitramine/GAP propellants was not observed. Profiles of species concentrations in flames of RDX/GAP and HMX/GAP propellants are similar; there are only some quantitative differences between them. Two zones of chemical reactions in flame of propellants based on GAP were detected. In the first (narrow, adjacent to the burning surface) flame zone with width of ~ 100 microns, complete consumption of nitramine vapor and NO_2 with formation of NO, CO, H_2 and N_2 occurs. In the second zone, consumption of N_2O, CH_2O, NO and HCN and formation of final products (CO, CO_2, N_2 and H_2) take place. It was shown that the same reactions (as in the case of pure nitramines) play lead role in nitramine/GAP propellant flames.

Experiments showed that there are carbonaceous particles on the burning surface upon combustion of nitramine/BAMO-AMMO propellants. In this case only one zone of chemical reaction in flame was observed.

The data obtained can be used to develop and validate a combustion model for propellants based on nitramines and azide polymers.

Reference.

1. O.P. Korobeinichev, “Flame Structure of Solid Propellants” Solid Propellant Chemistry, Combustion, and Motor Interior Ballistics, edited by Vigor Yang, Thomas B. Brill, and Wu-Zhen Ren.Vol. 185, Progress in Astronautics and Aeronautics, AIAA, New York , 2000, pp.335-354.
2. A.A. Zenin, “Experimental Investigation of the Burning Mechanism of Solid Propellants and Movement of Burning Products”, Ph.D. Dissertation, Inst. of Chemical Physics, USSR Academy of Sciences, Moscow, USSR, 1976.
3. A.G. Tereshenko, O.P. Korobeinichev, A.A. Paletsky, L.T. DeLuca, “Laser Support Ignition, Combustion and Gasification of AP-based Propellants”, The 8th International Workshop on Combustion and Propulsion, Pozzuoli, Naples, Italy, 16-20 June, 2002.
4. Korobeinichev O.P., Paletsky A.A., Volkov E.N., Tereschenko A.G., Polyakov P.D. “Investigation of Flame Structure of HMX/GAP Propellant at 0.5 Mpa” // Book of Proceedings of 9-IWCP "Novel Energetic Materials and Application" (Eds. L.T. DeLuca, L. Galfetti, and R. A. Pesce-Rodriguez), Grafiche GSS, Bergamo, Italy, paper 43, 2004.
5. J.L. Lyman, Y.-C. Liau, H.V. Brand, “Thermochemical Function for Gas-Phase, 1,3,5,7,-Tetranitro-1,3,5,7-tetraazacyclooctane (HMX), Its Condensed Phases, and Its Larger Reaction Products”, Combustion and Flame 130:185-203 (2002).
6. R. D. Schmidt, “Heats of formation of Energetic Oxetane Monomers and Polymers”, Energetic Materials *Ignition, Combustion and Detonation*, 32 International Annual Conference of ICT, Karlsruhe, Federal Republic of Germany, 2001, paper 140.
7. A.A. Zenin, “Study of Combustion Mechanism of Nitramine-Polymer Mixture,” Report No R&D 8724-AN-01, European Research Office of the US Army, 2000.
8. N. Kubota, T. Sonobe, "Burning Rate Catalysis of Azide/Nitramine Propellants," Proceedings of Twenty-third Symposium (International) on Combustion, Combustion Inst., Pittsburgh, PA, 1990, pp. 1331-1337.
9. Korobeinichev, O. P., Kuibida, L. V., Orlov, V. N., Tereshchenko, A. G., Kutsenogii, K. P., Mavliev, R. A., Emel'yanov, I. D., Ermolin, N. E., Fomin, V. M., "Mass spectrometric probe study of the flame structure and kinetics of chemical reactions in

flames", Mass-Spektrom. Khim. Kinet., Tal'roze, V. L (editor), 1985, pp. 73-93 (in Russian).

10. Korobeinichev O.P., Kuibida L.V., Madirbaev V. Zh., “Investigation of the Chemical Structure of the HMX Flame”, Comb. Explos. and Shock Waves, Vol. 20 No.3, 1984, p. 282.
11. Belov, G.V., “Astra” Code, ver. 2/24, MSTU, Moscow, 1990 (in Russian).
12. Y.J. Lee and T.A. Litzinger, “Thermal Decomposition of BAMO-AMMO with and without TiO2”, Thermochimica Acta 384 (2002) 121-135.
13. Korobeinichev O.P., Kuibida L.V., Paletsky A.A., Chernov A.A., "Study of Solid Propellant Flame Structure By Mass-Spectrometric Sampling", Combustion Science and Technology, 1996, Vols. 113-114, pp.557-571.
14. Simonenko V.N., Zarko V.E., Kiskin A.B., “Characterization of self-sustain combustion of cyclic nitramines”, Proceedings of 29th International Annual Conference of ICT, June 30-July 3, 1998, Karlsruhe, Germany, pp.169.
15. T.P. Parr and D.M. Hanson-Parr, “Solid Propellant Flame Structure”, Mat. Res. Soc. Symp. Proc. Vol. 418, 1996, pp. 207-219.
16. C.-J. Tang, Y.J. Lee, G. Kudva, T.A. Litzinger, “A Study of the Gas-Phase Chemical Structure During CO_2 Laser Assisted Combustion of HMX”, Combustion and Flame, Vol. 117, 1999, pp.170-188.
17. Zenin A.A., “HMX and RDX: Combustion Mechanism and Influence on Modern Double-Base Propellant Combustion”, *Journal of Propulsion and Power*, vol. 11, No 4, 1995, pp.752-739.

Tables and Figures

Table 1.
Characteristics of HMX and RDX

Name	HMX	RDX
Formula	$C_4H_8N_8O_8$	$C_3H_6N_6O_6$
Molecular weight, g/mole	296	222
Density, g/cm^3	1.9	1.81
Heat of formation, kcal/kg	71.0 [5]	76.6
Oxygen balance, % $O_2/CO_2,H_2O$	-21.6	-21.6

Table 2.
Characteristics of GAP and BAMO-AMMO copolymer

	GAP	BAMO-AMMO (B-A)
Name	Glycidyl azide polymer	(bis-azido-methyl-oxetane)-(azido-methyl-methyl-oxetane)
Formula	Monomer - $C_3H_5N_3O$ Brutto - $C_{60}H_{104}O_{21}N_{54}$ Number of hydroxyl groups - 2.58	Monomer BAMO $C_5H_8N_6O$ Monomer AMMO $C_5H_9N_3O$
Molecular weight, g/mole	1970 (average)	BAMO-AMMO copolymer (1:1) 1700(number average) 2700(weight average)
Density, g/cm^3	1.275	1.21
Enthalpy of formation, cal/g	146	284.2 [6]

Table 3.
The characteristics of the propellants nitramine/azide polymer (80/20 wt%)

	HMX/GAP	RDX/GAP	HMX/B-A	RDX/B-A
Brutto-formula	$C_{17.1}H_{32.5}N_{27.2}O_{23.8}$		$C_{17.6}H_{33.1}N_{27.7}O_{23.0}$	
Enthalpy of formation, cal/g	86	90.5	113.6	118.1
Density (TMD), g/cm^3	1.73	1.67	1.71	1.65
Density experim., g/cm^3	1.69±0.01	1.64±0.01	1.71±0.01	1.62±0.01
T_{ad}, K, P=1.0 MPa	2608	2617	2512	2522

Table 4

Species concentrations in flame of nitramine/GAP propellants at 0.5 and 1.0 MPa at different distances from the burning surface (in mole fractions).

	HMX/GAP P=0.5 MPa			HMX/GAP P=1.0 MPa			RDX/GAP P=1.0 MPa		
L, mm	0	~1.2	Equil.[a)]	0	~1.0	Equil.[a)]	0	~1.0	Equil.
T, K	603[c)]	2550[d)]	2594	638[c)]	2580[d)]	2608	638[c)]	2580[d)]	2617
H_2	0.04	0.23	0.225	0.12	0.23	0.226	0.12	0.23	0.225
H_2O	0.14	0.12	0.115	0.16	0.12	0.116	0.11	0.12	0.116
HCN	0.13	0	$<10^{-4}$	0.12	0	$<10^{-4}$	0.10	0	$<10^{-4}$
N_2	0.12	0.29	0.289	0.09	0.29	0.289	0.01	0.29	0.289
CO	0.02	0.34	0.335	0.12	0.34	0.336	0.11	0.34	0.336
NO	0.12	0	$<10^{-4}$	0.08	0	$<10^{-4}$	0.04	0	$<10^{-4}$
CH_2O	0.06	0	$<10^{-4}$	0.04	0	$<10^{-4}$	0.02	0	$<10^{-4}$
CO_2	0.03	0.03	0.027	0.02	0.03	0.027	~0.0	0.03	0.027
NO_2	0.11	0	$<10^{-4}$	0.05	0	$<10^{-4}$	0.09	0	$<10^{-4}$
N_2O	0.04	0	$<10^{-4}$	0.04	0	$<10^{-4}$	0.06	0	$<10^{-4}$
HMX_v	0.18	0	0	0.17	0	$<10^{-4}$		0	$<10^{-4}$
RDX_v							0.33		

[a)] equilibrium concentrations for H and OH radicals are not presented in the table;

[c)] surface temperature of propellant from Ref. [7];

[d)] corrected for heat loss by radiation.

Table 5.

Species concentrations in flame of HMX/B-A propellant at 0.5 MPa at different distances from the burning surface (in mole fractions).

	H_2	HCN	NO	N_2	CO	H_2O	CO_2	N_2O	HNCO	C_2N_2	CH_2N_2	CH_2O	HMX_v
1	0.02	0.17	0.25	0.11	0.12	0.19	0.024	0.087	0.012	0.006	0.006	0.02	0.004
2	0.066	0	0	0.385	0.27	0.23	0.04	0	0	0	0	0	0
3	0.25	0	0	0.288	0.345	0.09	0.02						

1 – near the burning surface (experiment);
2 – final combustion products (L ~ 1.5 mm, experiment);
3 – equilibrium composition of combustion products (calculations).

Table 6

Species concentrations in flame of HMX/B-A propellant at 1.0 MPa at different distances from the burning surface (in mole fractions) in comparison with those at 0.5 MPa

P, MPa	H_2	HCN	NO	N_2	CO	H_2O	CO_2	N_2O
near the burning surface								
0.5*	0.02	0.17	0.25	0.11	0.12	0.19	0.024	0.087
1.0	0.17	0.11	0.04	0.36	0.10	0.17	0.01	0.03
final combustion products								
0.5	0.066	0	0	0.385	0.27	0.23	0.04	0
1.0	0.12	0	0	0.42	0.28	0.15	0.03	0
1.0 (calc.)	0.25	0	0	0.288	0.345	0.09	0.02	0

* - concentration less than 0.02 are not presented

Table 7

Species concentrations in flame of RDX/B-A propellant at 1.0 MPa at different distances from the burning surface (in mole fractions).

P, MPa	H_2	HCN	NO	N_2	CO	H_2O	CO_2	N_2O
near the carcass of RDX/B-A								
1.0	0.05	0.15	0.17	0.22	0.12	0.22	0.02	0.05
final combustion products RDX/B-A								
1.0	0.09	0	0	0.48	0.3	0.12	0.02	0
1.0 (calc.)	0.25	0	0	0.288	0.345	0.09	0.02	0

Table 8.

Composition of species (in mole fractions) near the burning surface of HMX at 0.1 MPa.

	r_b, mm/s	H_2	HCN	NO	N_2	CO	H_2O	CO_2	N_2O	NO_2	CH_2O	HMX_v
	0.65	0.04	0.1	0.26	0.1	0.09	0.22	0.02	0.07	0.03	0.03	0.04
*	0.9	0.01	0.19	0.14	0.09	0.18	0.14	0	0.1	0.11	0.06	-

* - C.-J. Tang et al., laser-induced combustion of HMX, 100W/cm^2 [16]

Table 9.

Composition of RDX combustion products near the burning surface at different conditions (in mole fraction)

p, MPa	H_2	HCN	NO	N_2	CO	H_2O	CO_2	N_2O	HNCO	NO_2	CH_2O	RDX_v
0.1	0.05	0.17	0.23	0.05	0.12	0.17	0.03	0.04	identif.	0.05	0.01	0.07

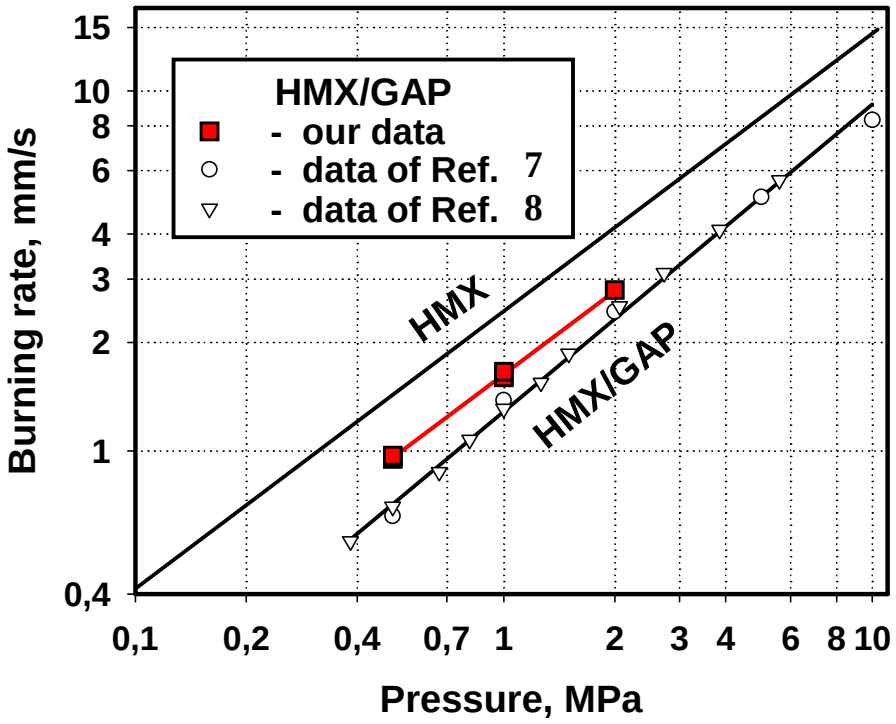

Fig. 1. Burning rate of HMX/GAP propellant in comparison with burning rate of pure HMX.

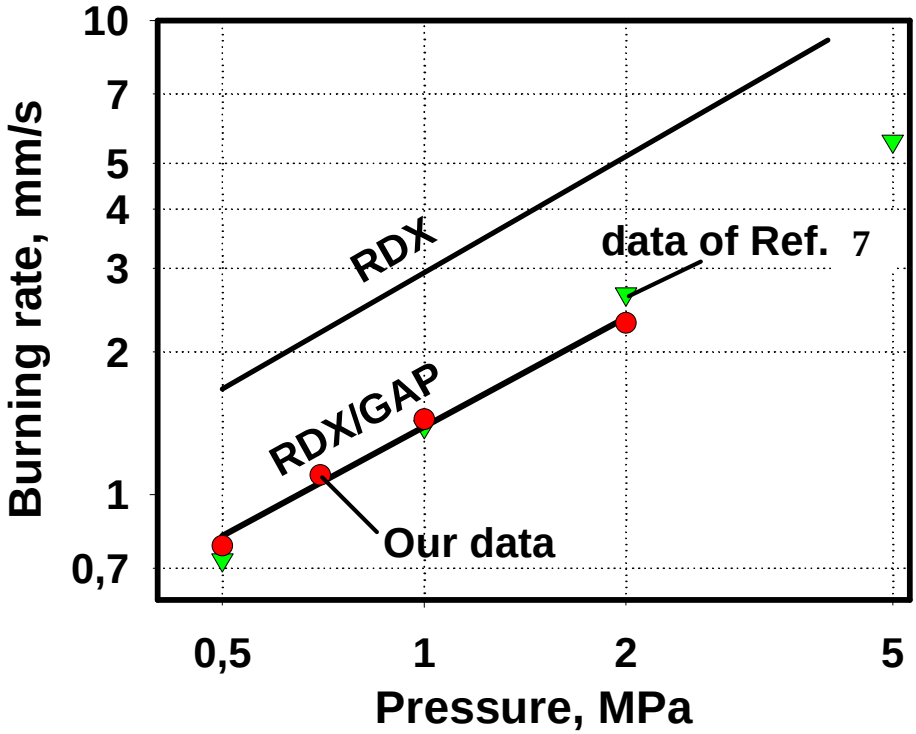

Fig. 2. Burning rate of RDX/GAP propellant in comparison with burning rate of pure RDX.

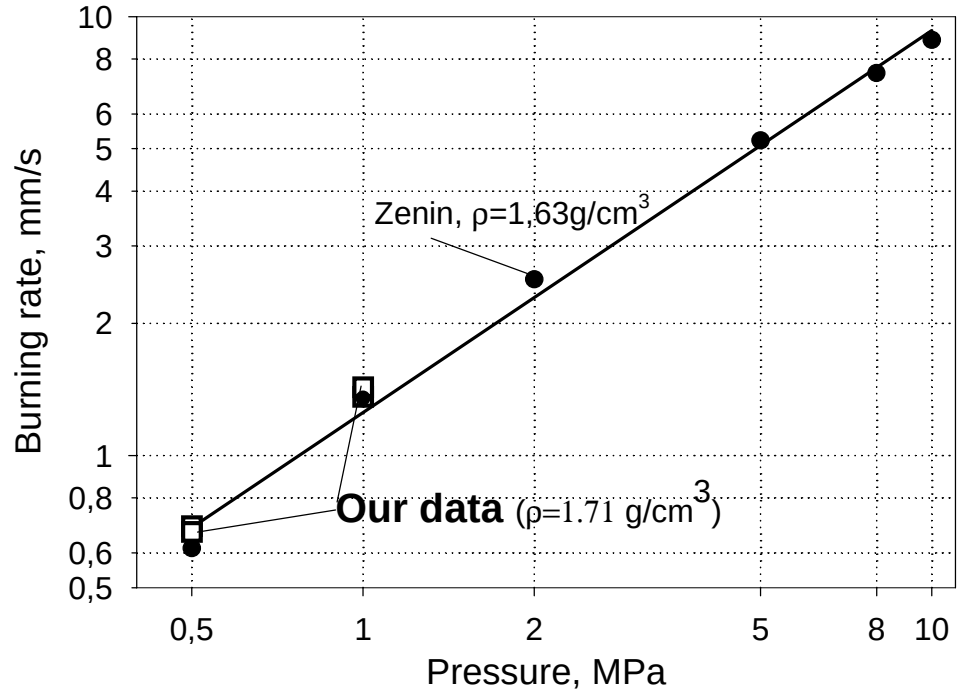

Fig. 3. Burning rate of HMX/BAMO-AMMO propellant in comparison with literature data.

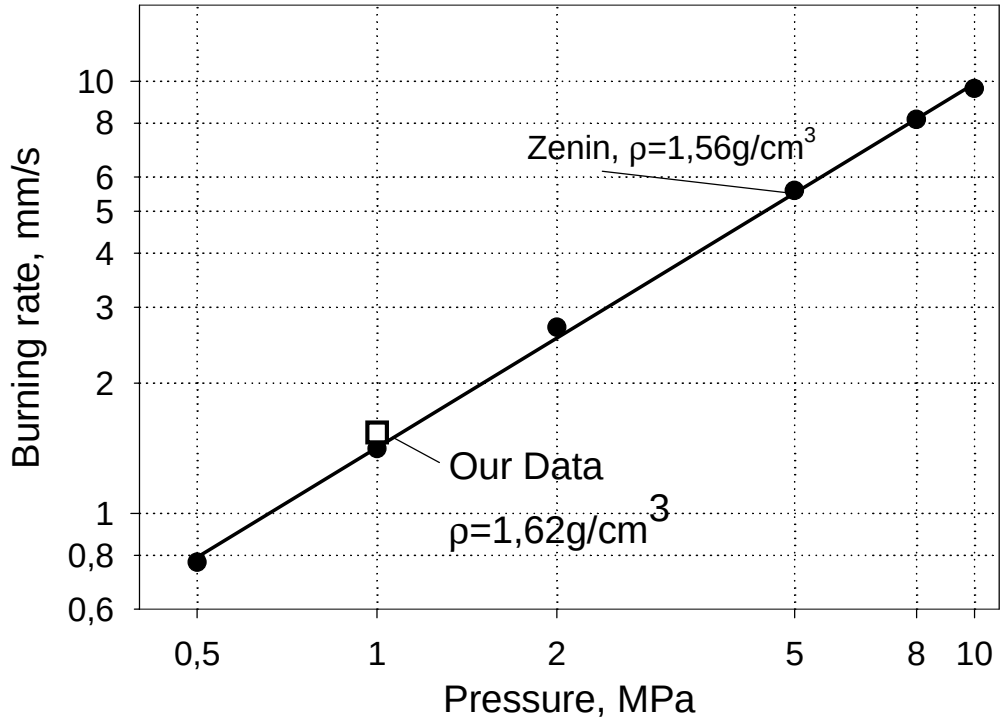

Fig.4. Burning rate of RDX/BAMO-AMMO propellant in comparison with literature data.

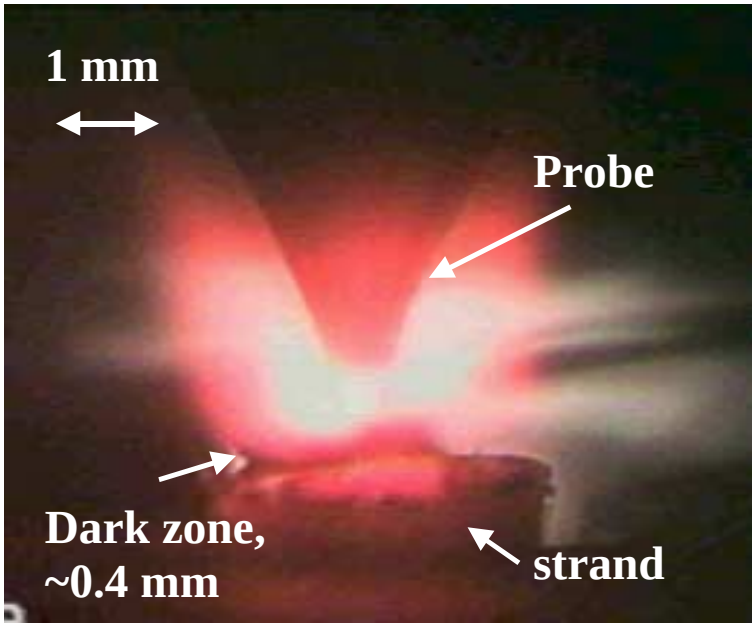

Fig. 5. The dark zone near the burning surface of the HMX/GAP propellant at 0.5 MPa

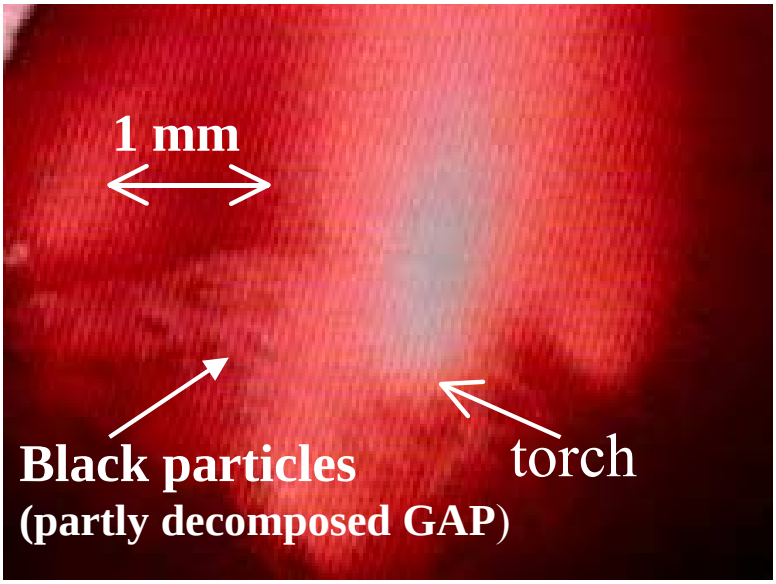

Fig.6. Burning surface of HMX/GAP propellant at 0.5 MPa

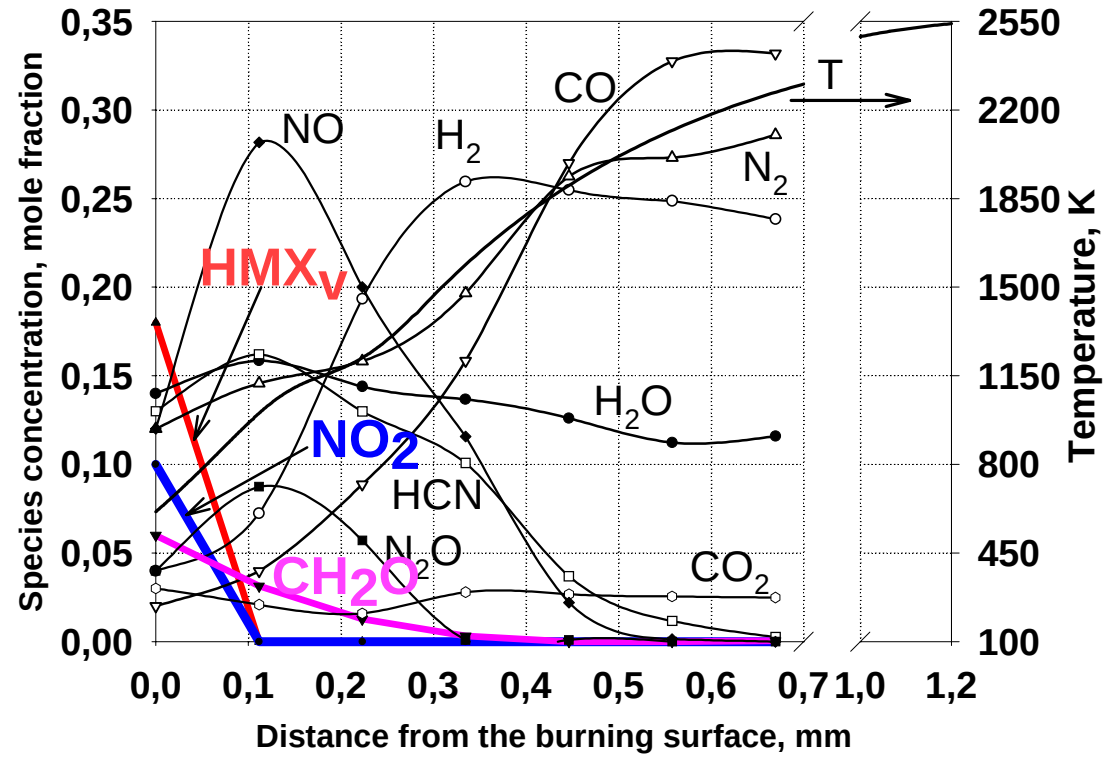

a)

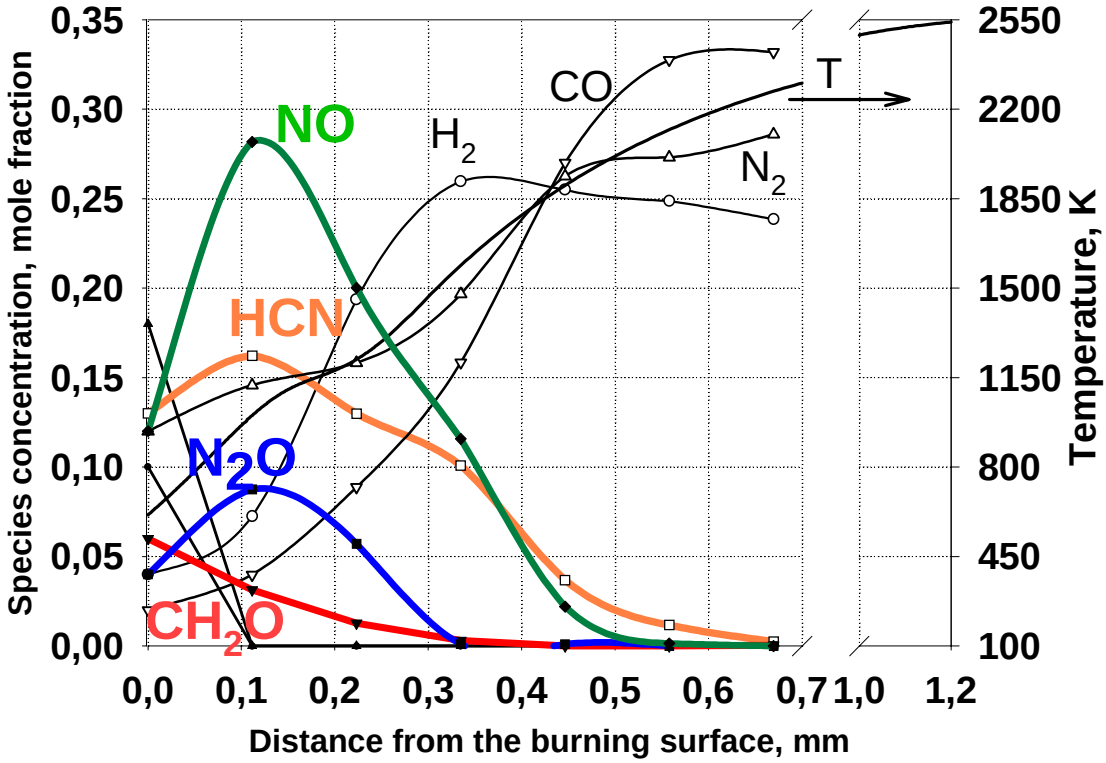

b)

Fig.7 (a, b). HMX/GAP flame structure at 0.5 MPa

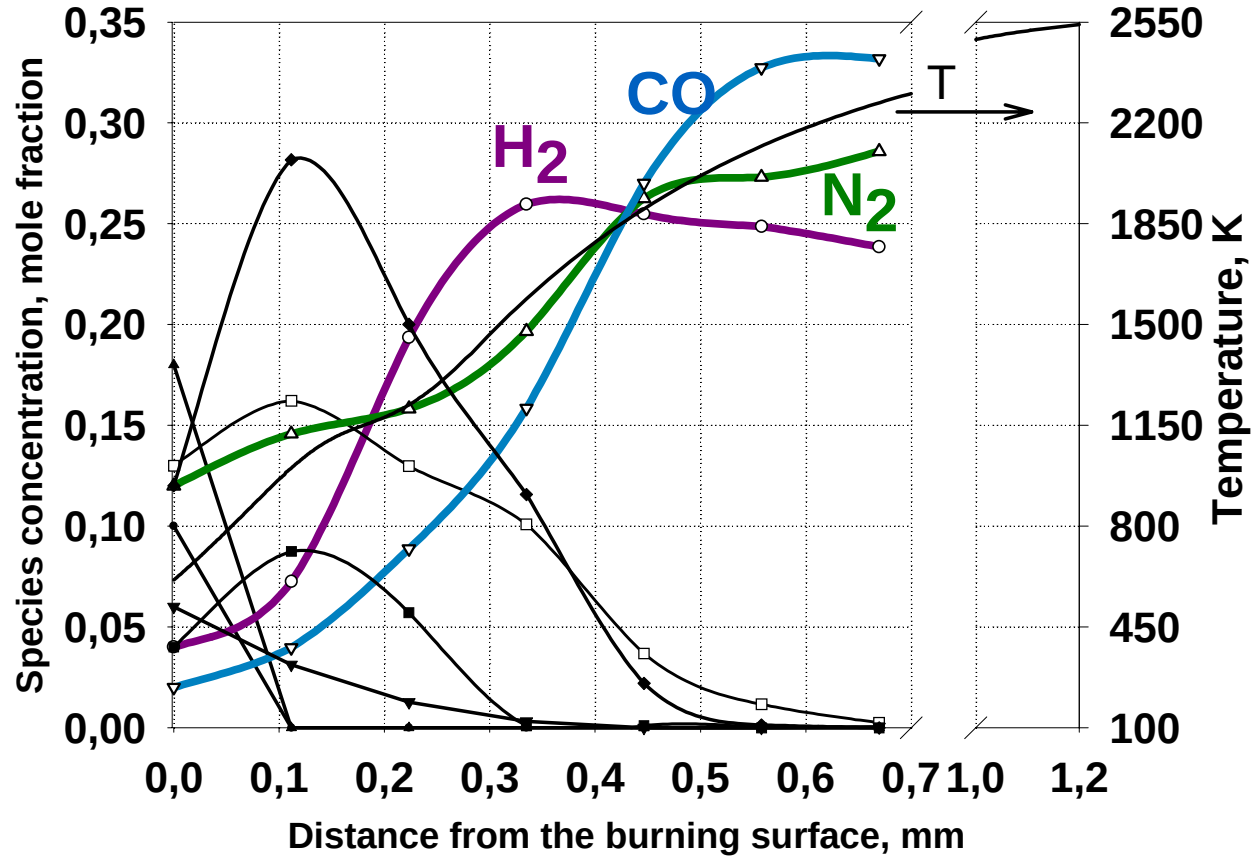

c)

Fig. 7 (c). HMX/GAP flame structure at 0.5 MPa

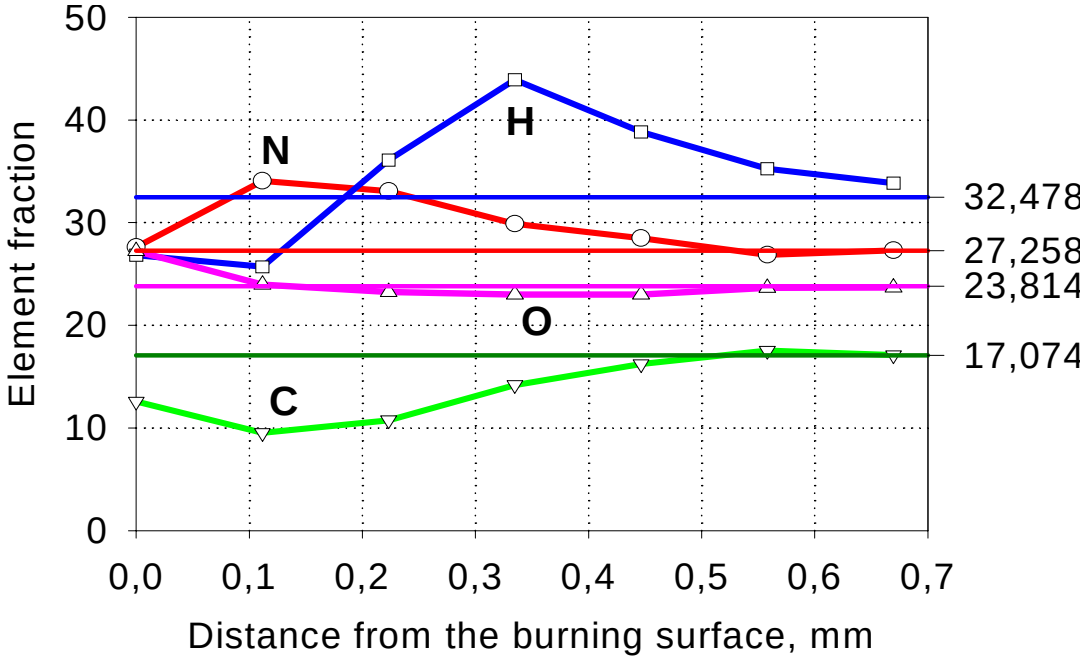

Fig. 8 Element content profiles in HMX/GAP propellant flame at 0.5 MPa

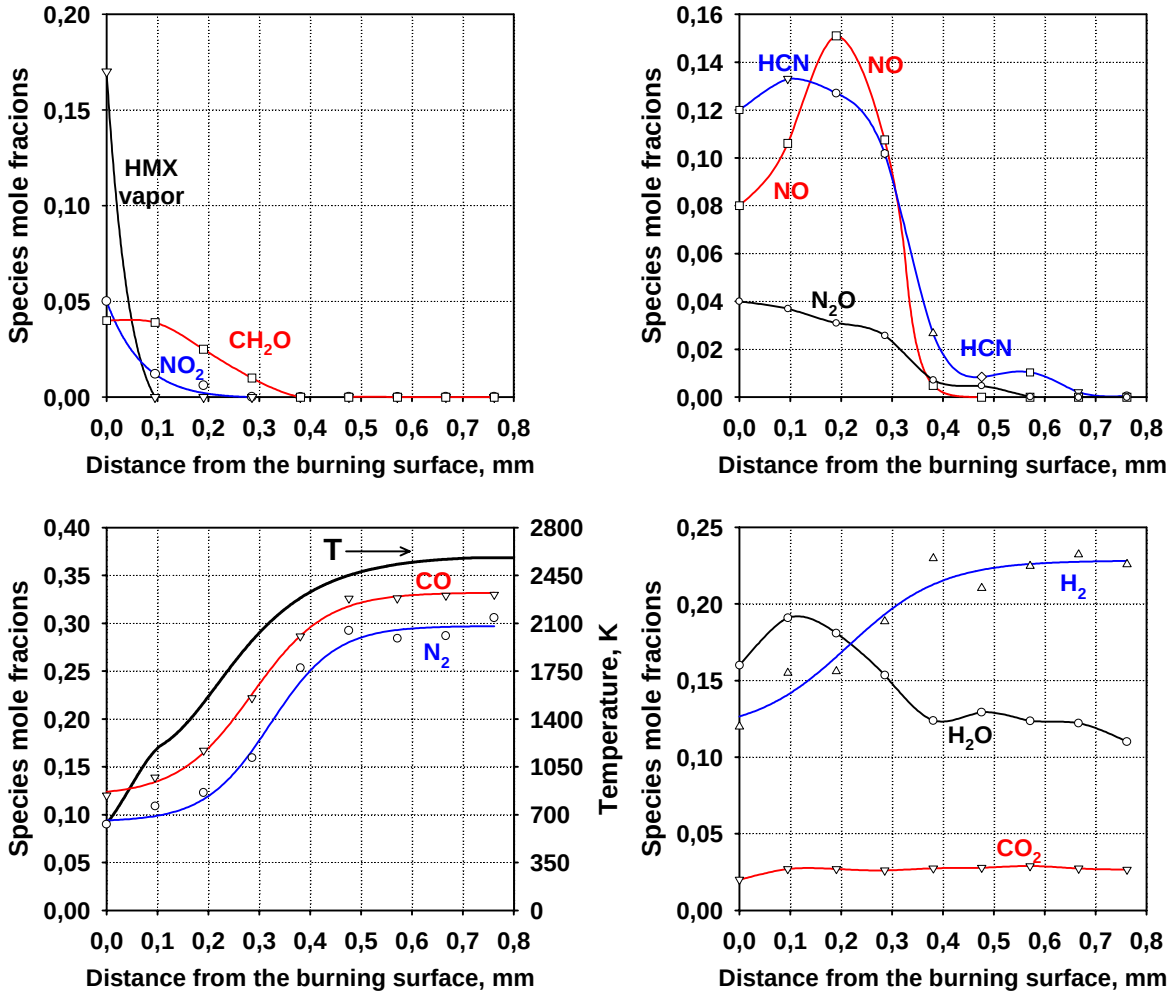

Fig. 9. Flame structure of HMX/GAP propellant at a pressure of 1 MPa

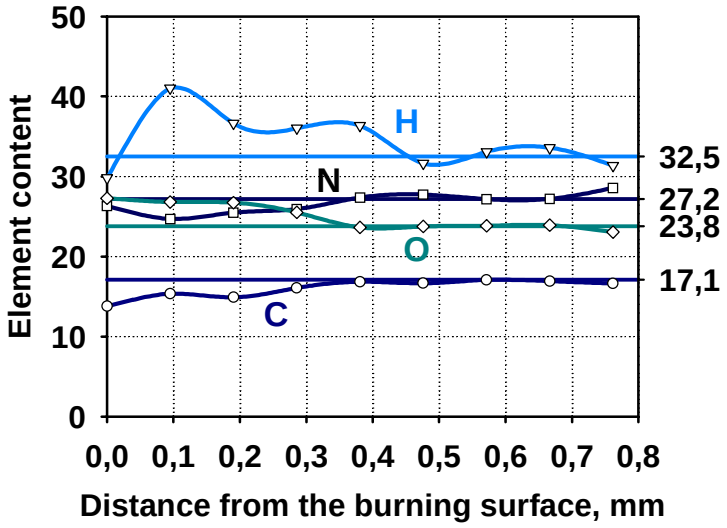

Fig. 10. Element content profiles in HMX/GAP propellant flame at 1 MPa.

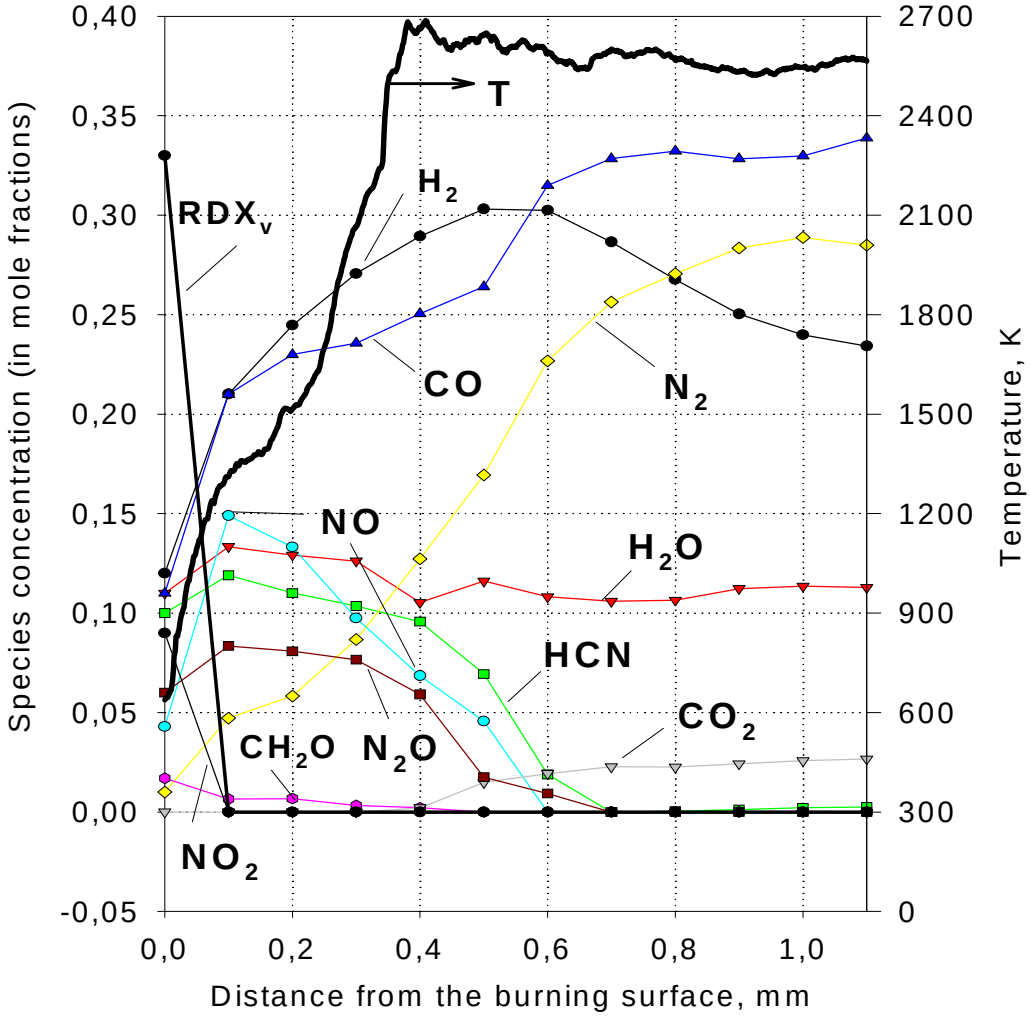

Fig. 11. Flame structure of RDX/GAP propellant at 1 MPa.

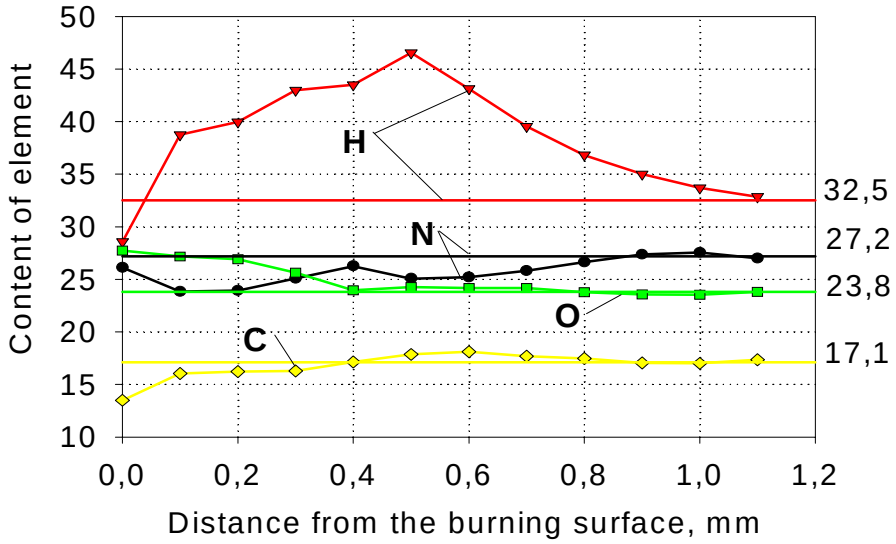

Fig. 12. Element content profiles in RDX/GAP propellant flame at 1 MPa.

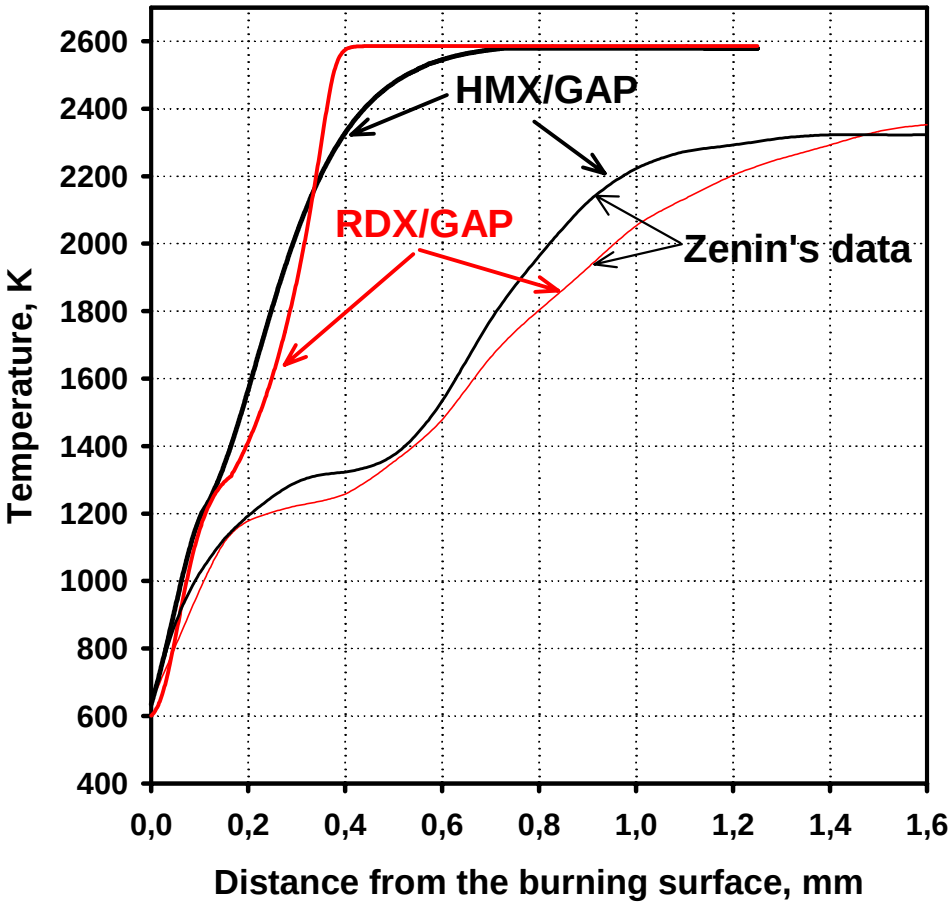

Fig. 13. Temperature profiles in flames of nitramine/GAP (80/20) propellants at a pressure of 1MPa.

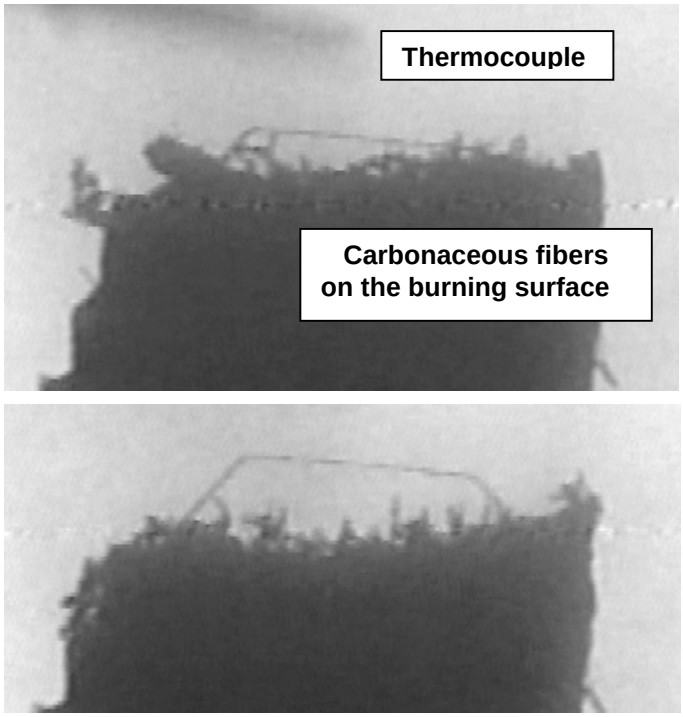

a) P=0.5 MPa

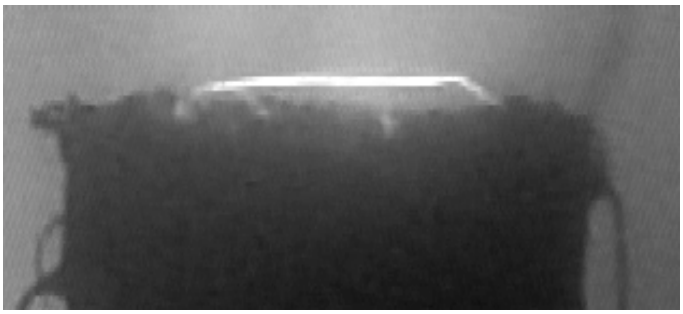

b) P=1.0 MPa

Fig.14. The burning of cured HMX/GAP propellant at different pressures.

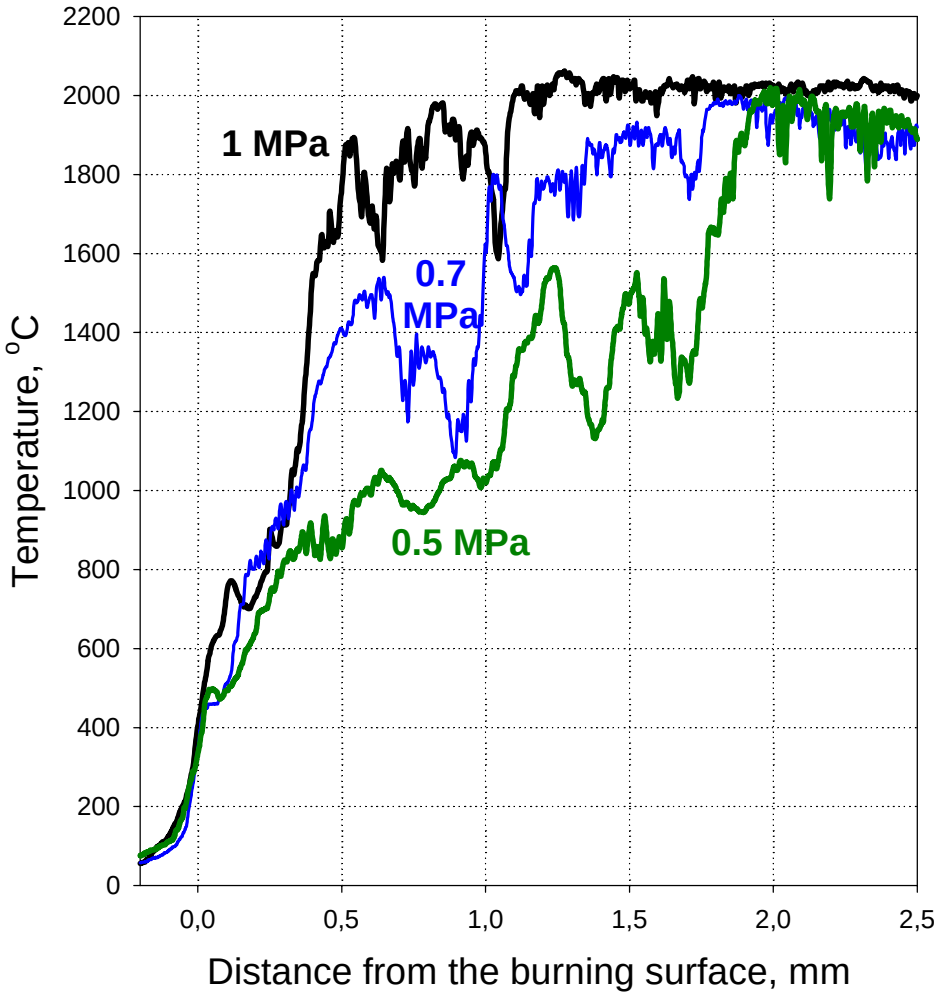

Fig.15. Temperature profiles (without correction for heat losses by radiation) in flame of cured HMX/GAP propellant at different pressures.

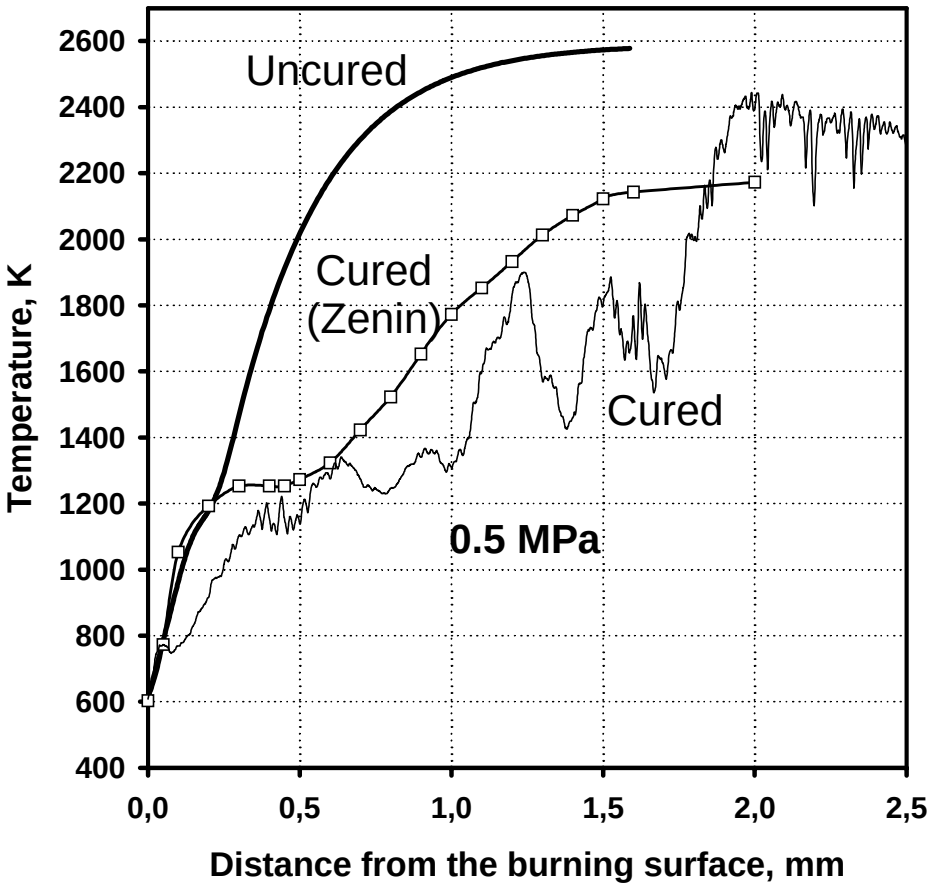

Fig.16. Temperature profiles in flame of HMX/GAP propellant at 0.5 MPa: uncured propellant, cured propellant and Zenin's profile for cured propellant [7].

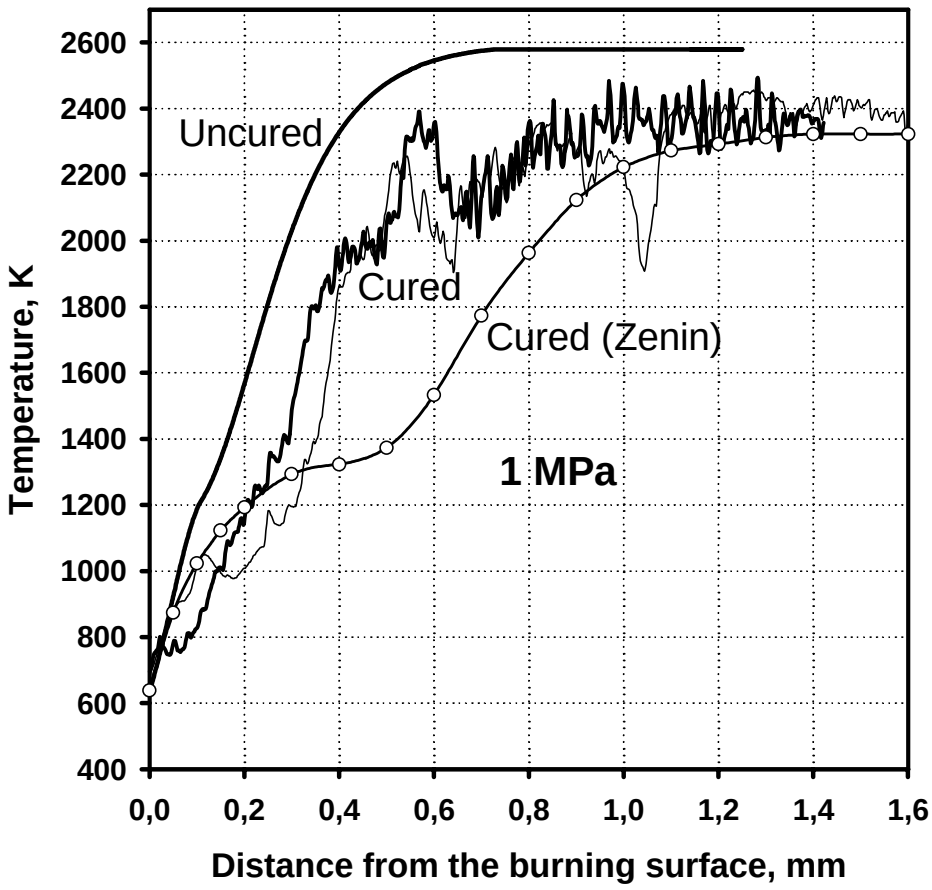

Fig.17. Temperature profiles in flame of HMX/GAP propellant at 1.0 MPa: uncured propellant, cured propellant and Zenin's profile for cured propellant [7].

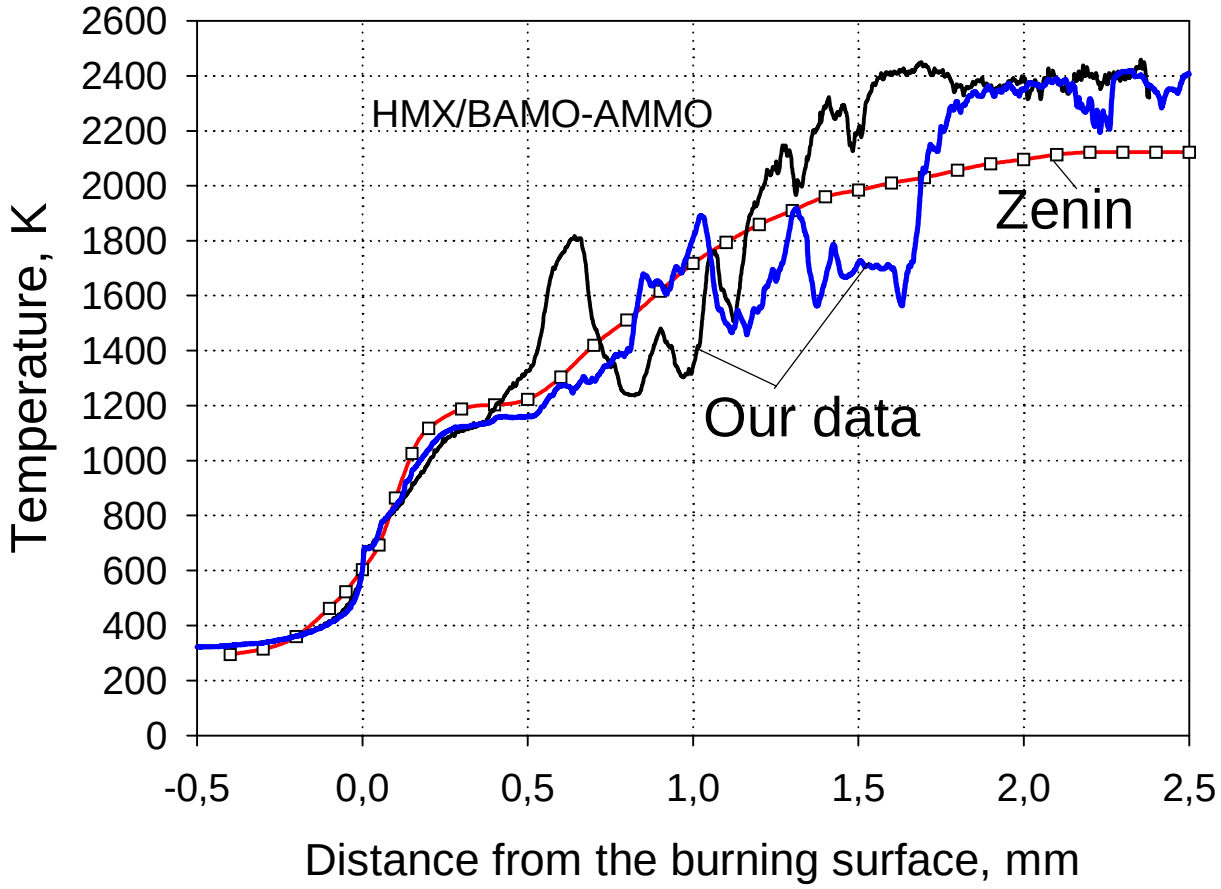

Fig.18. Temperature profiles in HMX/B-A combustion wave at a pressure of 0.5 MPa (corrected for heat losses by radiation; obtained in different experiments).

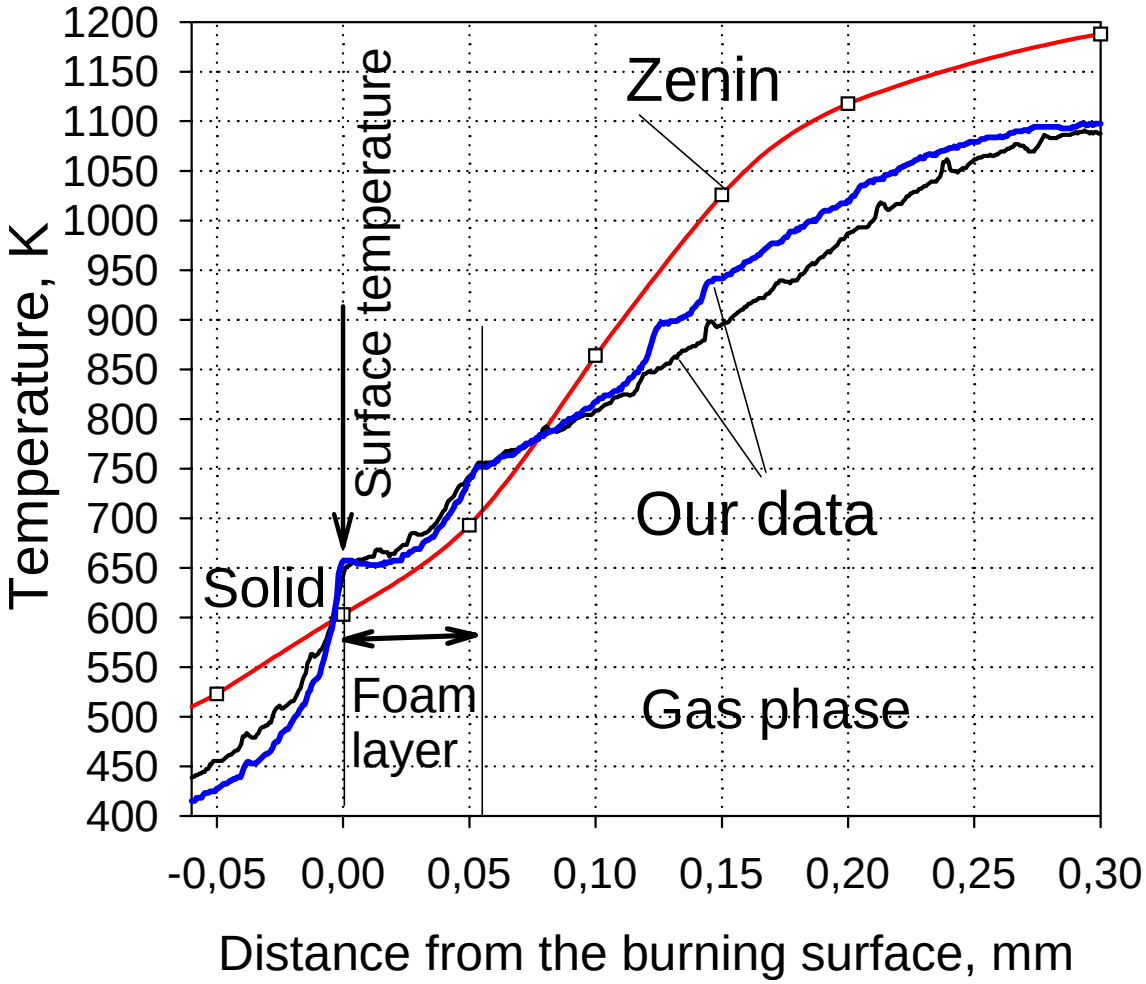

Fig.19. Temperature profiles near the burning surface of HMX/B-A propellant at a pressure of 0.5 MPa (obtained in different experiments).

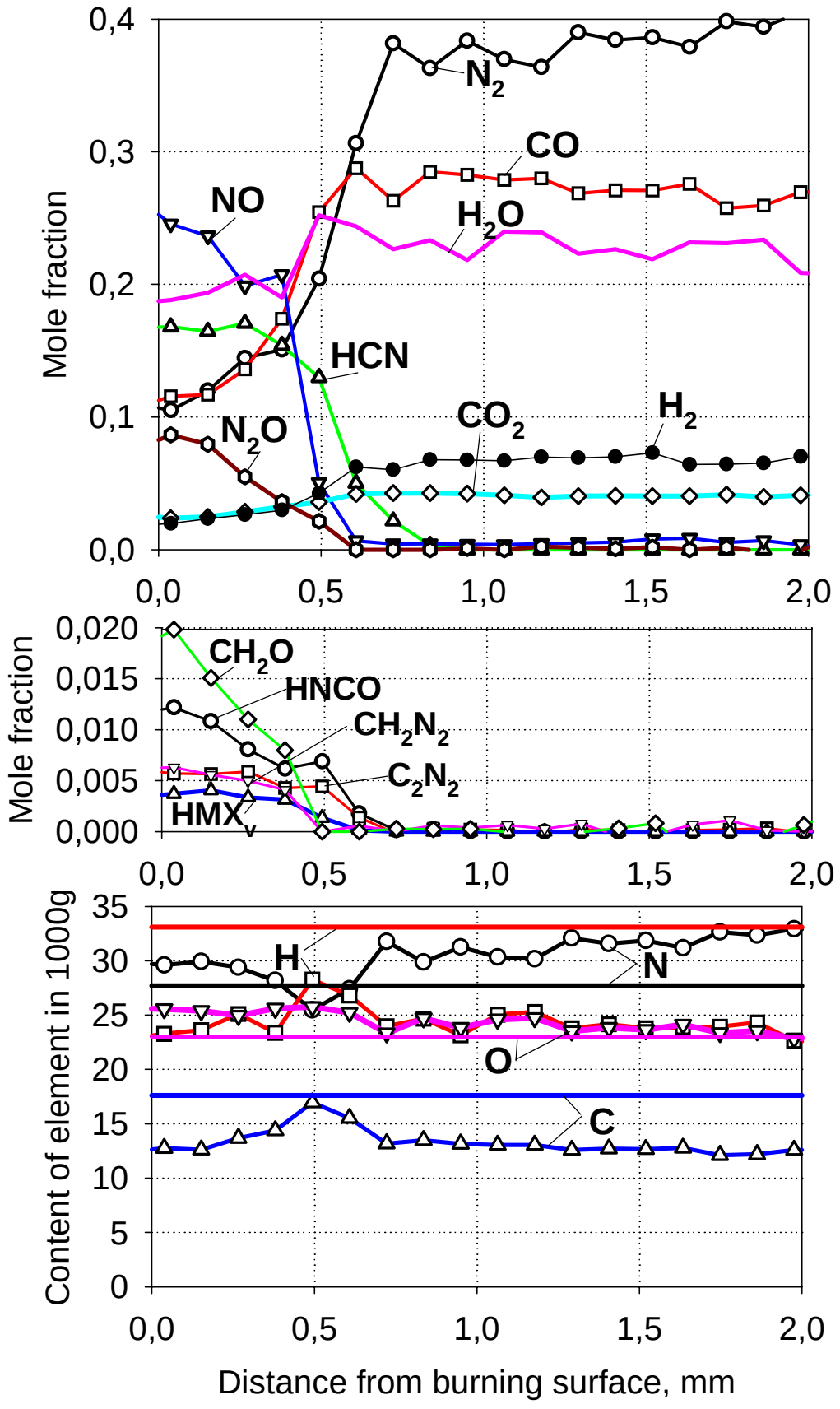

Fig.20. Flame structure of HMX/B-A propellant at 0.5 MPa.

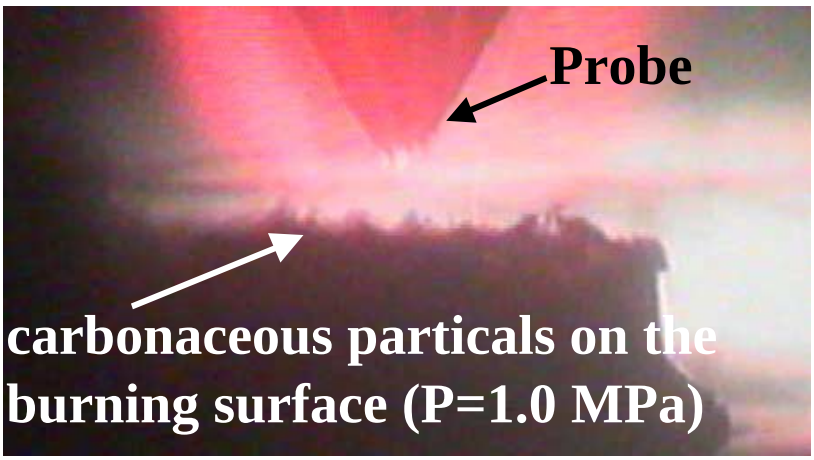

a) HMX/BAMO-AMMO

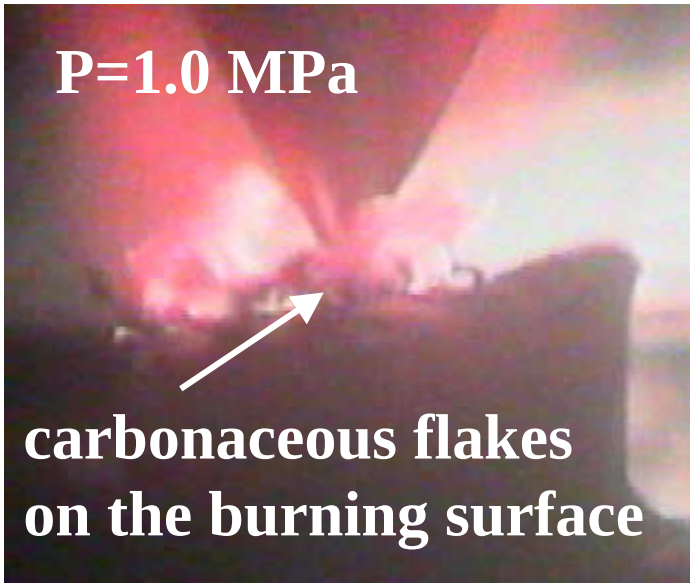

b) RDX/BAMO-AMMO

Fig. 21. The burning surface of BAMO-AMMO-based propellants at a pressure of 1 MPa.

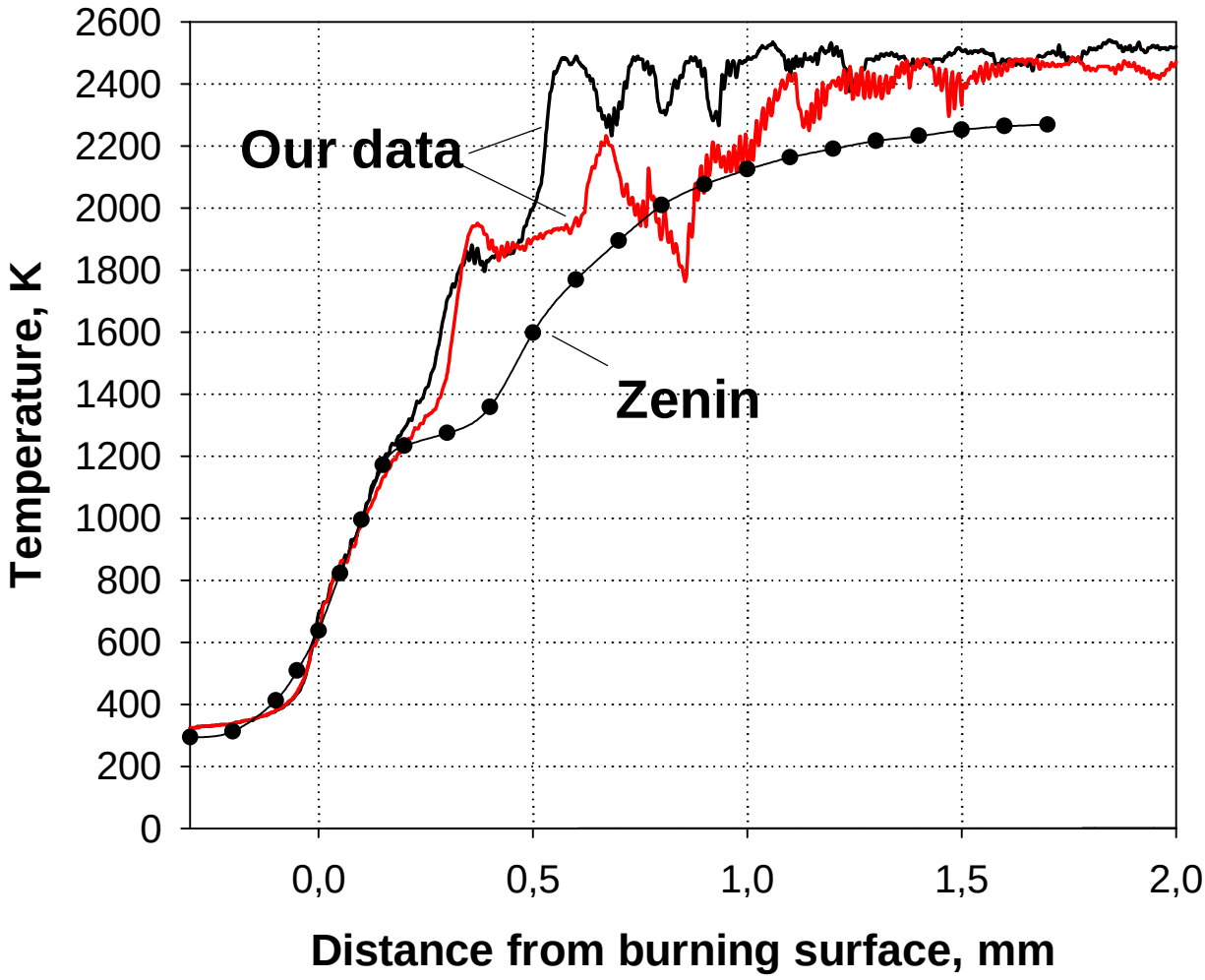

Fig. 22. Temperature profiles in HMX/B-A combustion wave at a pressure of 1 MPa (corrected for heat losses by radiation; obtained in different experiments).

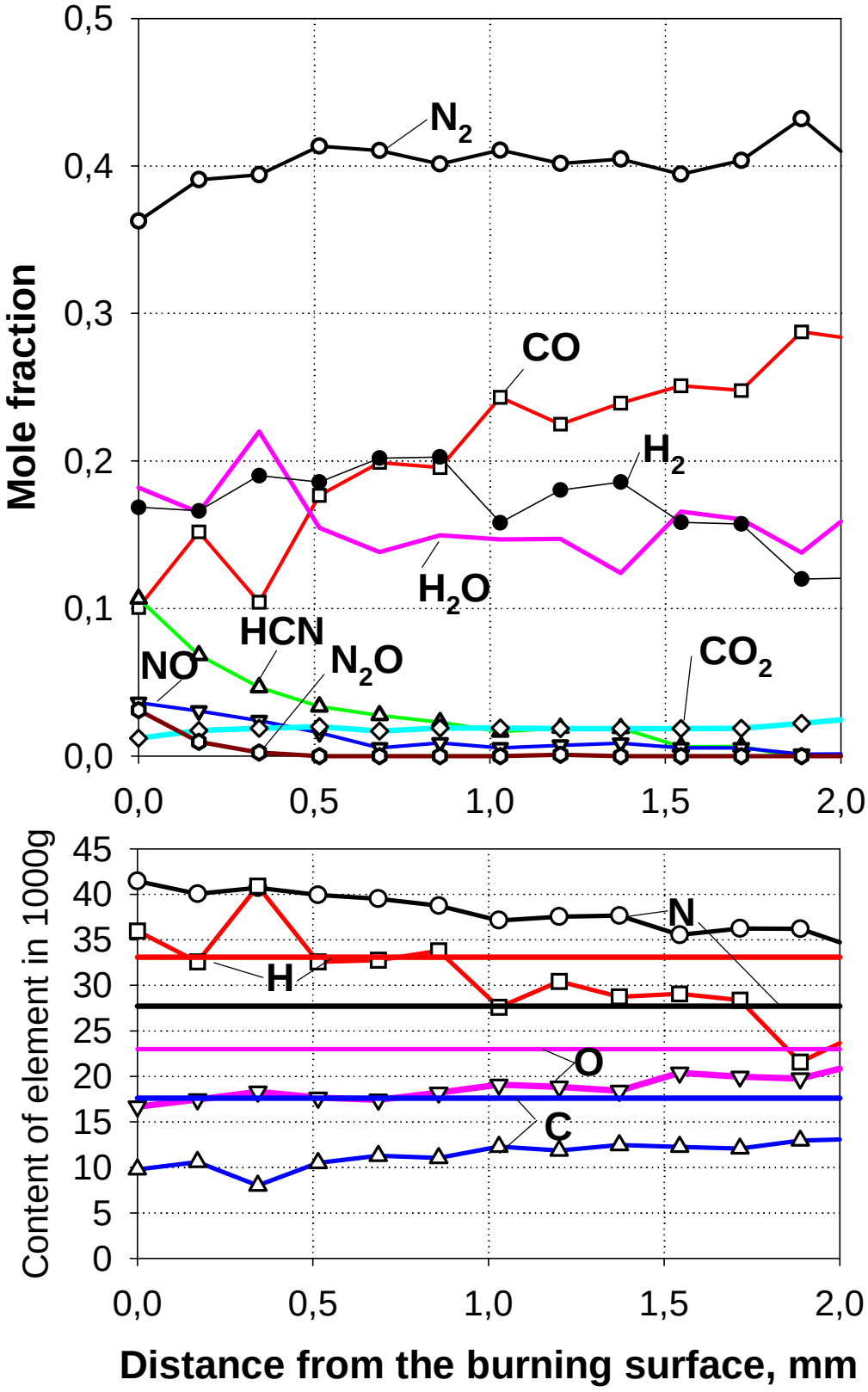

Fig. 23. Flame structure of HMX/B-A propellant at 1 MPa.

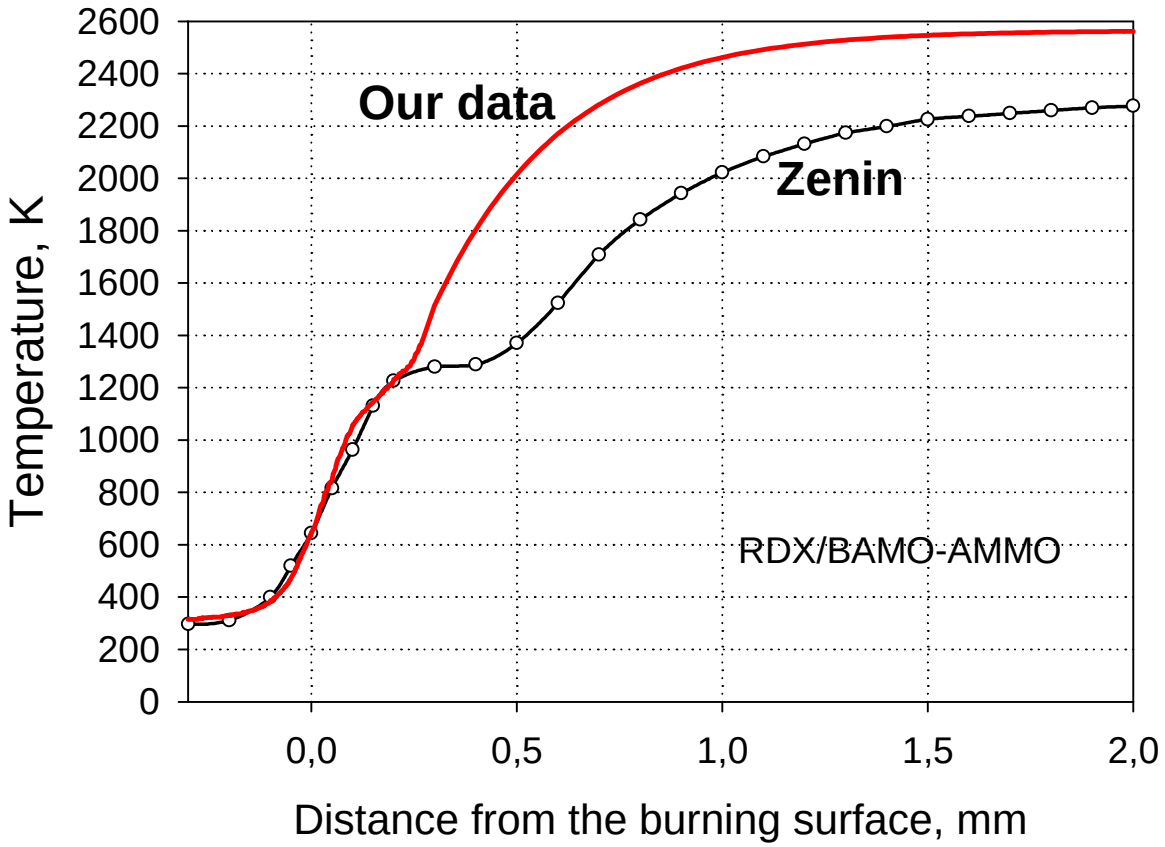

Fig. 24. Temperature profiles in RDX/B-A combustion wave at a pressure of 1 MPa (corrected for heat losses by radiation).

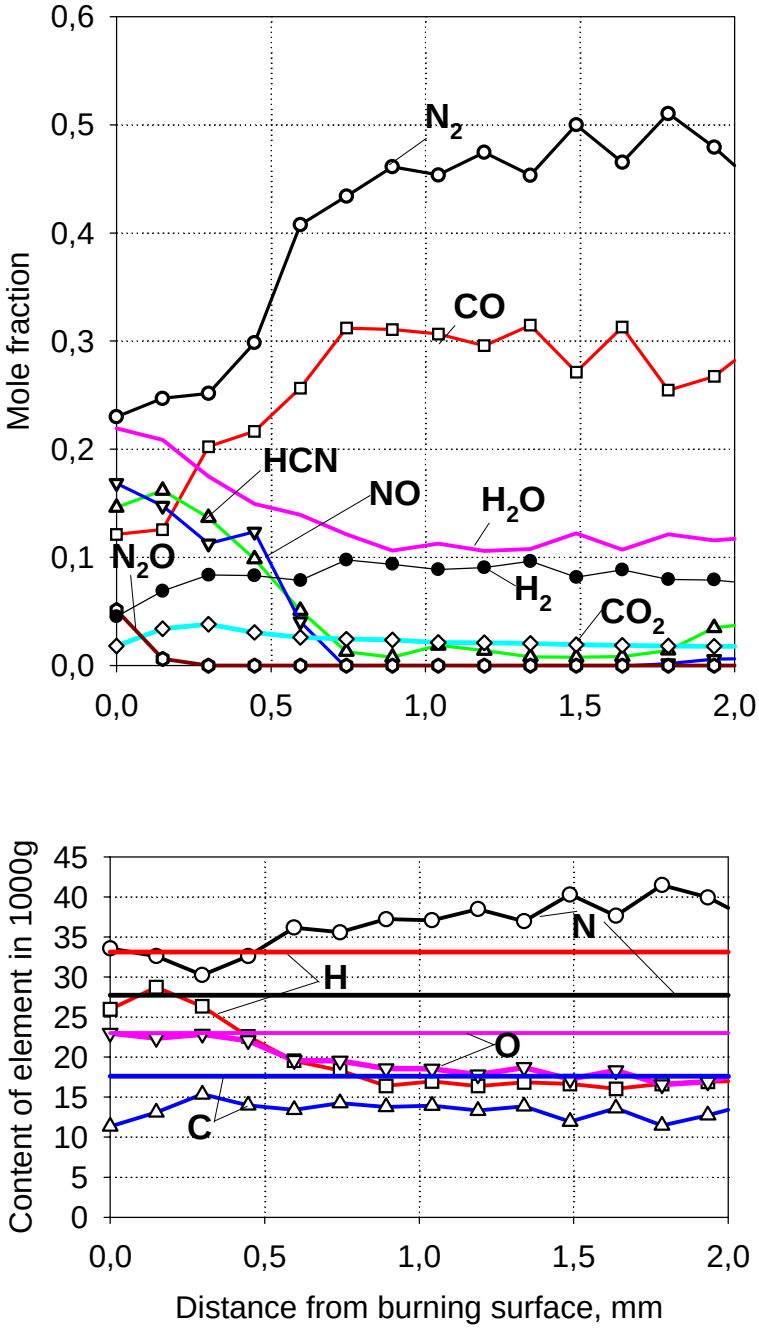

Fig. 25. Flame structure of RDX/B-A propellant at 1 MPa.

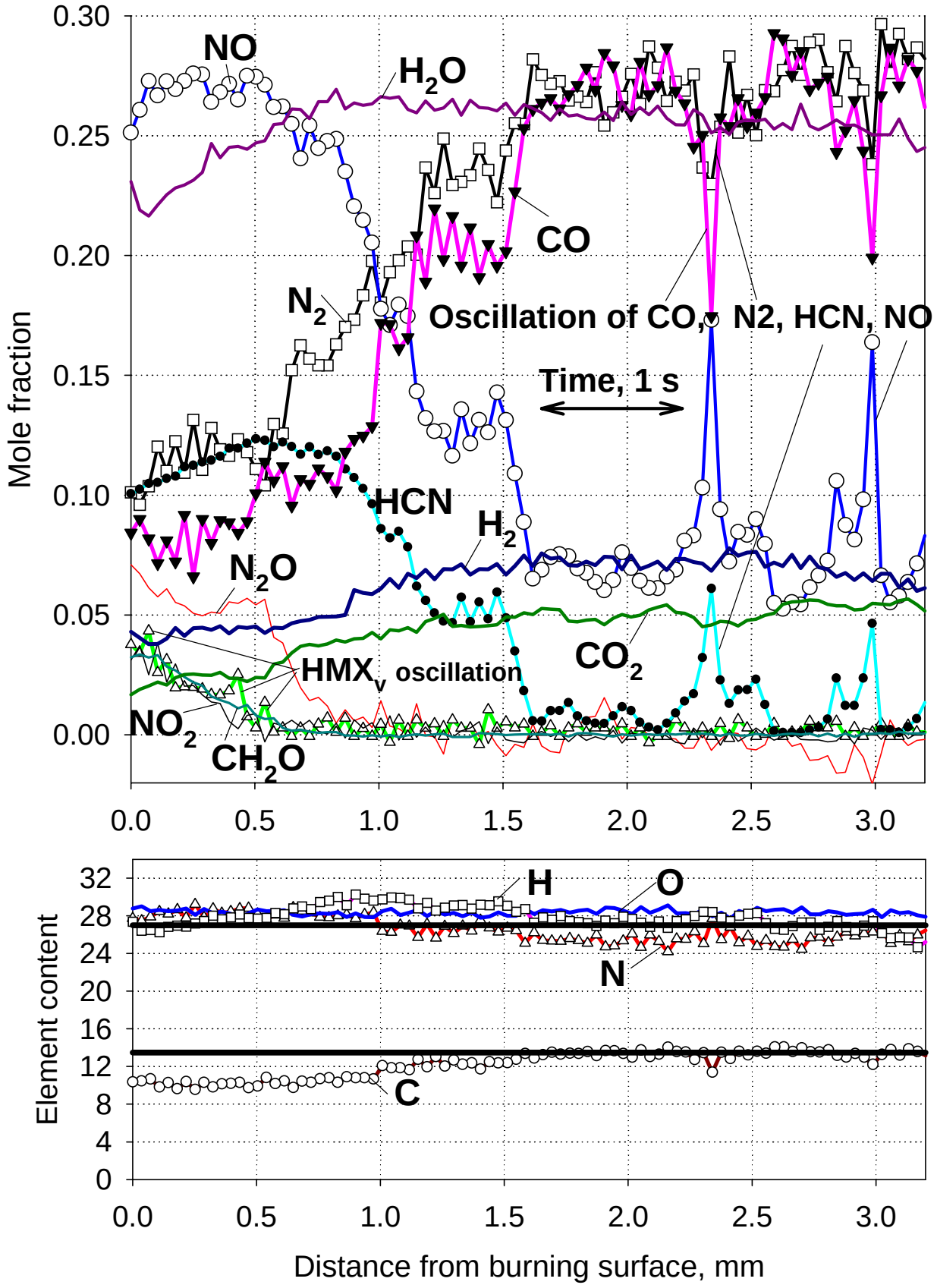

Fig. 26. Flame structure of HMX at 0.1 MPa (ambient air).

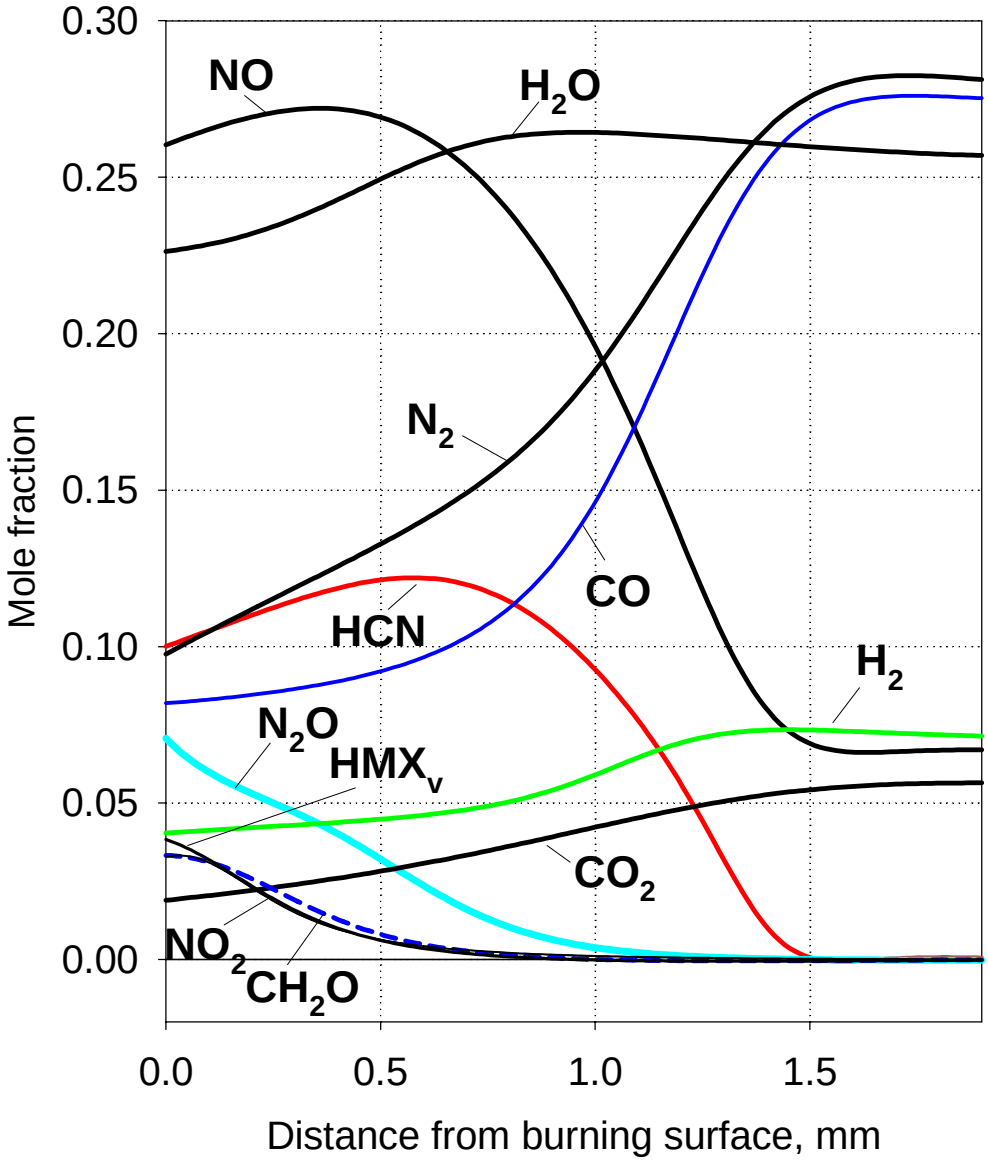

Fig.27. Flame structure of HMX at 0.1 MPa (ambient air).

Averaged smoothed data.

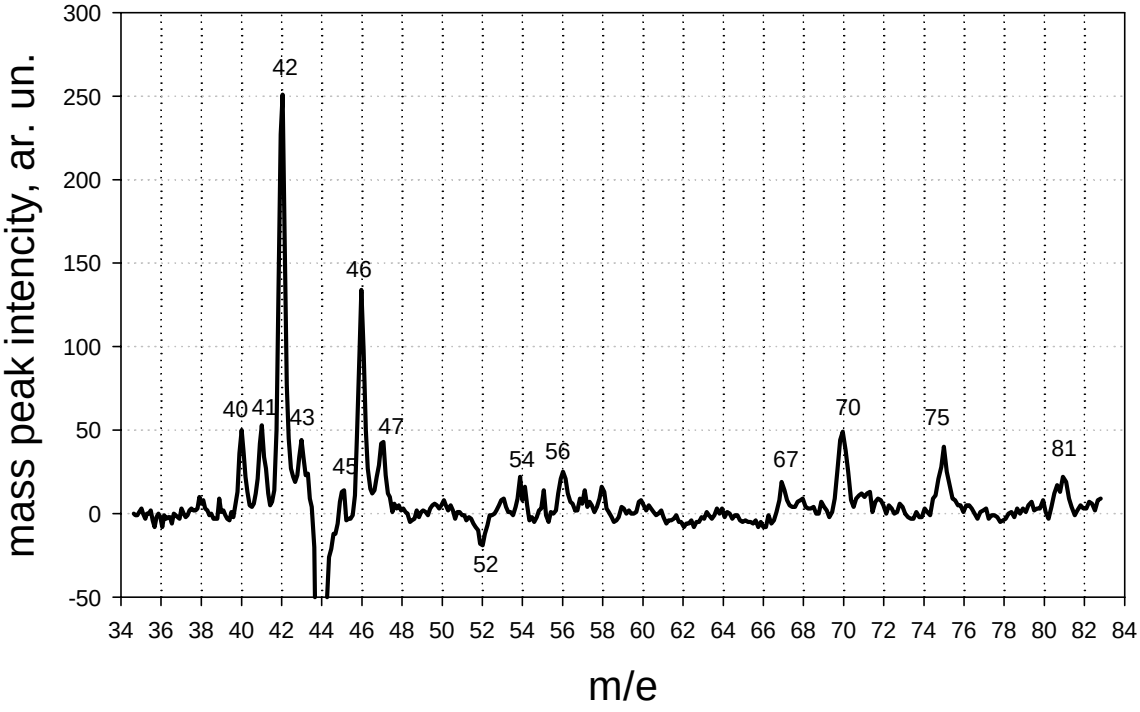

Fig. 28. Result of subtraction of mass spectrum of combustion products in the end of the first zone of HMX flame at 0.1 MPa (at a distance of ~ 0.5 mm) from mass spectrum of products near the burning surface.

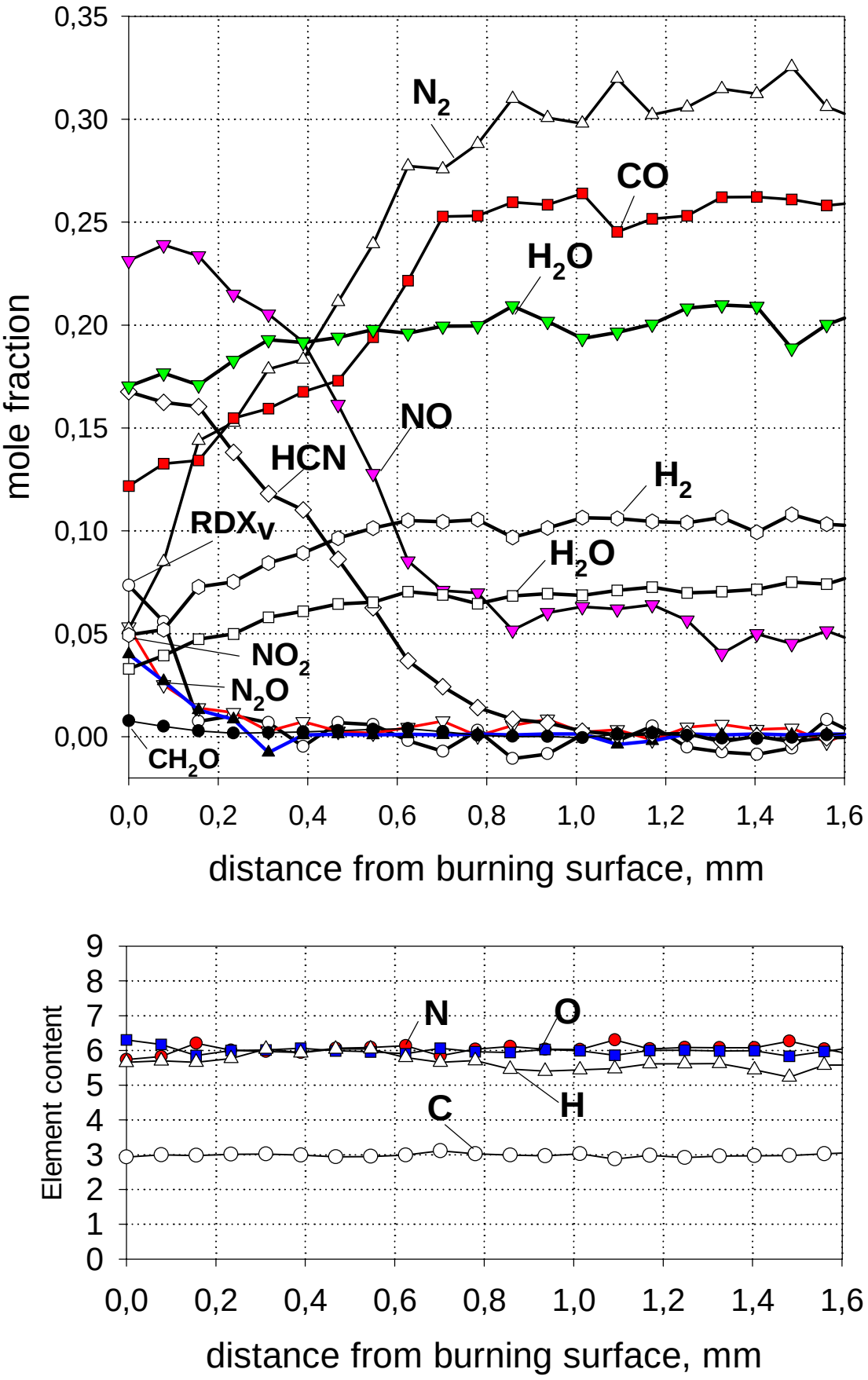

Fig. 29. Flame structure of RDX at 0.1 MPa in argon.

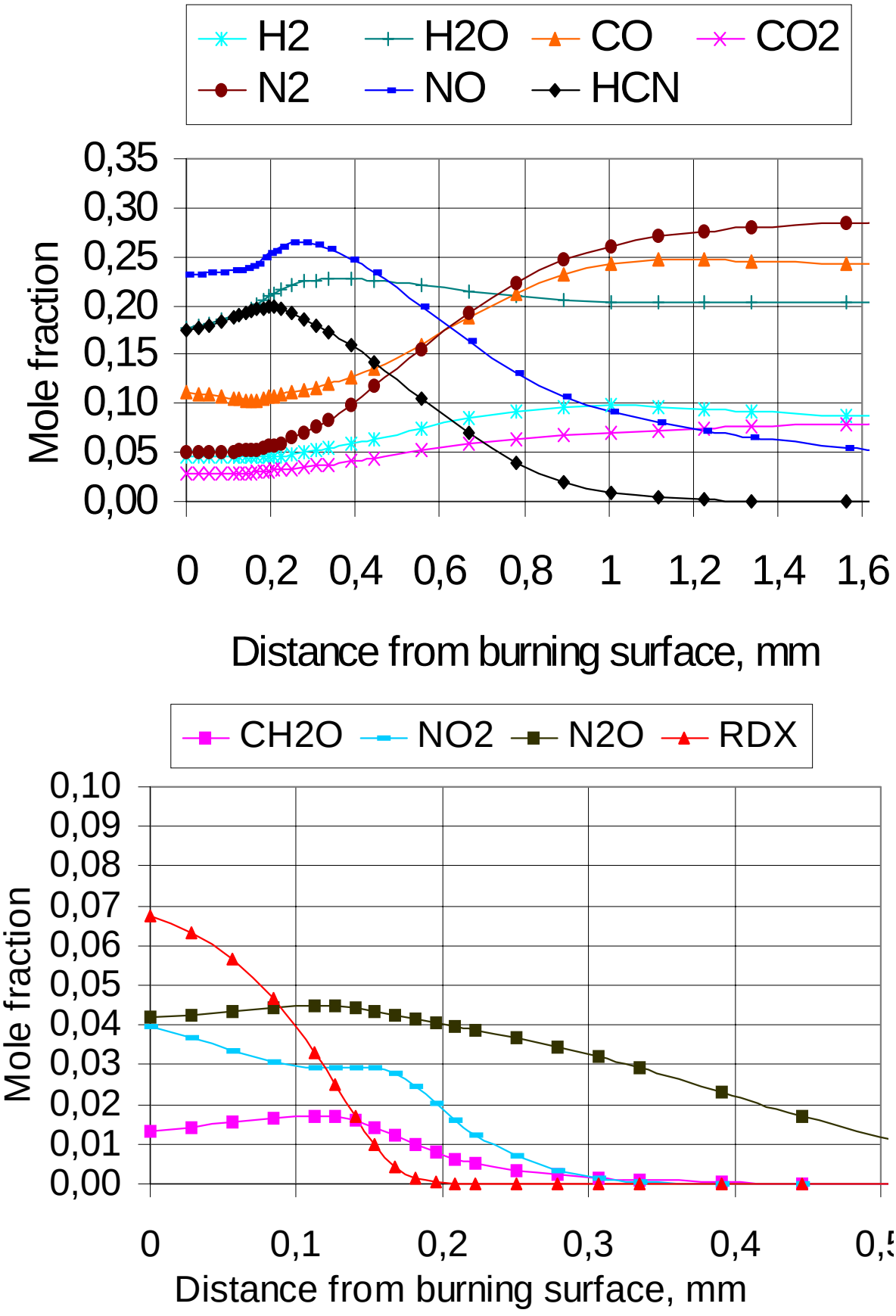

Fig. 30. Modeling of RDX flame at 0.1 MPa.

List of Publications supported ARO under this grant

(6)a Papers published in peer-reviewed journals

1. Korobeinichev O.P., Paletsky A.A., Volkov E.N., Tereschenko A.G., Polyakov P.D. "Investigation of Flame Structure of HMX/GAP Propellant at 0.5 Mpa" // Book of Proceedings of 9-IWCP "Novel Energetic Materials and Application" (Eds. L.T. DeLuca, L. Galfetti, and R. A. Pesce-Rodriguez), Grafiche GSS, Bergamo, Italy, paper 43, 2004.
2. Paletsky A.A., Korobeinichev O.P., Tereshchenko A.G., Volkov E.N., Polyakov P.D. "Flame structure of HMX/GAP propellant at high pressure" // Proceedings of the Combustion Institute (Editors: Barlow R.S., Colket M.B., Chen J.H., Yetter R.A.), vol.30 #2, pp.2102-2109, Elsevier, 2004
3. Korobeinichev O.P., "Study of Energetic Material Combustion Chemistry by Probing Mass Spectrometry and Modeling of Flame", in Book "Overviews of Recent Research on Energetic Materials" (Editors - R.W. Shaw, T.B. Brill, D.L.Thompson), Advanced Series in Physical Chemistry, vol.16, World Scientific Publishing Co. Pte. Ltd., Singapore, 2005, pp. 75-103.

6(b) Papers published in non-peer-reviewed journals or in conference proceedings

1. Korobeinichev O.P., Paletsky A.A., Volkov E.N., Tereshchenko A.G., Polyakov P.D., T.A. Bolshova, "Combustion Chemistry and Flame Structure of Cyclic Nitramine and Composite Propellants Based on Them", Proceedings of All-Russian conference "Advances in special chemistry and chemical technology", Part II, 8-10 June 2005, Moscow, Russia, pp. 46-50 (in Russian).
2. P.D. Polyakov, O.P. Korobeinichev, A.A. Paletsky, E.N. Volkov, A.G. Tereshchenko "Investigation of RDX flame structure at atmospheric pressure using probing mass-spectrometry and modeling", Proceedings of the European Conference for Aerospace Sciences, July 4-7, 2005, Moscow, Russia, CD version.
3. P.D. Polyakov, O.P. Korobeinichev, A.A. Paletsky, E.N. Volkov, A.G. Tereshchenko "Investigation of RDX flame structure at atmospheric pressure using probing mass-spectrometry and modeling", European Combustion Meeting, April 3-6, 2005, Louvain-la-Neuve Belgium, CD version.

4. Volkov E.N., Paletsky A.A., Tereshchenko A.G., Polyakov P.D., Korobeinichev O.P., "Investigation of Flame Structure of Composite Propellants Based on Nitramines and Glycidyl Azide Polymer at a Pressure of 10 atm Using Probing Molecular Beam Mass Spectrometry", 5th International Seminar on Flame Structure, 11-14 July, 2005, Novosibirsk, Russia.

(6)c Paper presented at meeting, but not published in conference proceedings

1. O.P. Korobeinichev, A.A. Paletsky, A.G. Tereshchenko, E.N. Volkov, P.D. Polyakov, "Molecular Beam Mass Spectrometry as Perspective Method for Diagnostics of Flames of condensed Systems", *International Conference on Combustion and Detonation, Ze'ldovich Memorial*, August 30 – September 3, 2004, Moscow, Russia.
2. Volkov E.N., Paletsky A.A., Tereshchenko A.G., Polyakov P.D., Korobeinichev O.P., "Investigation of flame structure of composite propellants based on nitramines and glycidyl azide polymer at pressures of 5-10 atm using probing molecular beam mass spectrometry", Book of Abstracts *Second International Workshop-school "Mass Spectrometry in Chemical Physics, Biophysics and Environmental Sciences"*, October, 4-7, 2004, Moscow, Russia, p.147.
3. Korobeinichev O.P., "Flame Structure Study by Molecular Beam Mass-Spectrometry", Book of Abstracts *Second International Workshop-school "Mass Spectrometry in Chemical Physics, Biophysics and Environmental Sciences"*, October, 4-7, 2004, Moscow, Russia, p. 173.
4. Polyakov P.D., Volkov E.N., Paletsky A.A., Korobeinichev O.P., "Measurement of Mass-Spectrum of Vapor of Energetic Materials at Atmospheric Pressure by Molecular Beam Mass-Spectrometry", Book of Abstracts *Second International Workshop-school "Mass Spectrometry in Chemical Physics, Biophysics and Environmental Sciences"*, October, 4-7, 2004, Moscow, Russia, p.274.
5. Volkov E.N., Paletsky A.A., Tereshchenko A.G., Polyakov P.D., Korobeinichev O.P., "Investigation of Flame Structure of Composite Propellants Based on Nitramines and Glycidyl Azide Polymer at a Pressure of 10 atm Using Probing Molecular Beam Mass Spectrometry", XIII (Russian) Symposium on Combustion and Explosion, Chernogolovka, Russia, 7-11 February, 2005.

6. Paletsky A.A., Volkov E.N., Polyakov P.D., Tereshchenko A.G., Korobeinichev O.P, "Investigation of RDX Flame Structure at Atmospheric Pressure Using Probing Mass Spectrometry", XIII (Russian) Symposium on Combustion and Explosion, Chernogolovka, Russia, 7-11 February, 2005.

List of participating scientific personnel showing any advanced degrees

1. Volkov E.N. – Doctor of Philosophy
2. Polyakov P.D. – Master of Physics